

2014-07-28

Enhanced Optical and Electrical Properties of Organic Field Effect Transistor using Metal Nanoparticles

Seongman Cho

University of Miami, choseongman0422@hotmail.com

Follow this and additional works at: https://scholarlyrepository.miami.edu/oa_theses

Recommended Citation

Cho, Seongman, "Enhanced Optical and Electrical Properties of Organic Field Effect Transistor using Metal Nanoparticles" (2014). *Open Access Theses*. 502.

https://scholarlyrepository.miami.edu/oa_theses/502

This Open access is brought to you for free and open access by the Electronic Theses and Dissertations at Scholarly Repository. It has been accepted for inclusion in Open Access Theses by an authorized administrator of Scholarly Repository. For more information, please contact repository.library@miami.edu.

UNIVERSITY OF MIAMI

ENHANCED OPTICAL AND ELECTRICAL PROPERTIES OF ORGANIC FIELD
EFFECT TRANSISTOR USING METAL NANOPARTICLES

By

Seongman Cho

A THESIS

Submitted to the Faculty
of the University of Miami
in partial fulfillment of the requirements for
the degree of Master of Science

Coral Gables, Florida

August 2014

©2014
Seongman Cho
All Rights Reserved

UNIVERSITY OF MIAMI

A thesis submitted in partial fulfillment of
the requirements for the degree of
Master of Science

ENHANCED OPTICAL AND ELECTRICAL PROPERTIES OF ORGANIC FIELD
EFFECT TRANSISTOR USING METAL NANOPARTICLES

Seongman Cho

Approved:

Sung Jin Kim, Ph.D.
Professor of Electrical Engineering

Michael Wang, Ph.D.
Professor of Electrical Engineering

Weizhao Zhao, Ph.D.
Professor of Biomedical Engineering

M. Brian Blake, Ph.D.
Dean of the Graduate School

CHO, SEONGMAN

(M.S., Electrical and Computer Engineering)

Enhanced Optical and Electrical Properties of Organic
Field Effect Transistor using Metal Nanoparticles.

(August 2014)

Abstract of a thesis at the University of Miami.

Thesis supervised by Professor Sung Jin Kim.

No. of pages in text. (56)

Organic field effect transistors (OFETs) have several advantages over the conventional inorganic field effect transistor such as easy fabrication process, low-cost mass production capability and low temperature process that enables flexible substrate based device. Many applications using polymer based transistor devices are demonstrated. Successful demonstrations of Logic-gate operation, visible-IR detection and various sensor operations and the advantages discussed above show its great potential as a next generation device technology and attract many researchers to delve to improve the device properties. However, there are several disadvantages on the organic materials such as short lifetime, disability to operate under severe conditions and low carrier mobility. Among those the low carrier mobility is a critical hurdle to develop high performance device operation. Its low mobility limits the operation speed of the device, efficient amplification and carrier transport in a detector device.

In this thesis, hybrid organic transistors using Poly(3-hexylthiophene-2,5-diyl)(P3HT) and metal nanostructure are introduced. The metal nanostructure has a unique localized surface plasmon resonance property that can be tailored by adjusting the shape and size of the metal structures. Therefore, the hybridization using polymer semiconducting materials and metal nanoparticles can provide plasmon based optical response and

improved mobility due to the free electron concentration in the metal nanostructure. We fabricated organic thin film transistor on a highly doped silicon substrate and characterized its electrical properties as a transistor operation and optical detection properties as a field effect transistor based detector. Then, metal nanoparticles have been deposited by vacuum evaporation of small molecules on the surface of the OFETs. The electrical and optical properties have been investigated to compare with a device without plasmonic nanostructure. We successfully demonstrated the improved optical properties of the OFETs are due to surface plasmon resonance of the metal nanoparticles. The metal nanoparticles incorporated in organic transistor shows improved drain current due to the increased conductivity assisted by the free electrons in the metal nanoparticles. In addition, we observed enhanced photo responsivity (A/W) in its optical detector operation. A slight change of the spectral response was observed and we believe that this is originated from the contribution of the plasmon induced hot electrons in the metal nanoparticles. Further studies to have better understandings on metal nanoparticle incorporated in organic transistor were discussed in this thesis.

TABLE OF CONTENTS

	Page
LIST OF FIGURES	iv
Chapter	
1 INTRODUCTION	1
2 BACKGROUND	7
Organic Semiconductor	7
Organic Field Effect Transistor (OFET).....	16
Surface Plasmon Resonance (SPR)	18
3 FABRICATION and CHARACTERISTICS of OFET	24
Fabrication of OFET	24
Optical Properties of OFET	27
Electrical Properties of OFET.....	34
4 OFET with METAL NANOPARTICLES	37
Metal Nanoparticles	37
Fabrication of Gold Nanoparticles incorporated in Organic Transistor	39
5 EXPERIMENTAL RESULT	43
Enhanced Optical Properties.....	43
Enhanced Electrical Properties	49
6 SUMMARY and FUTURE WORK	51
Summary	51
Important Consideration and Future Work	52
REFERENCES	54

LIST OF FIGURES

Figure 2.1 The shapes of orbitals depending on the symmetrical axis of rotation in three-dimensional space. (a), s orbital. (b), p_x orbital, p_y orbital and p_z orbital.	8
Figure 2.2 Energy diagram for 1s, 2s, $2p_x$, $2p_y$ and $2p_z$ orbitals.	8
Figure 2.3 Formation of a Sigma bond. (a), A covalent bond resulting from the $\sigma(s-s)$ formation of a molecular orbital by the end-to-end overlap of s type atomic orbitals. (b), A covalent bond resulting from the $\sigma(p-p)$ formation of a molecular orbital by the end-to-end overlap of p type atomic orbitals. (c), A covalent bond resulting from the $\sigma(s-p)$ formation of a molecular orbital by the end-to-end overlap of s and p type orbitals.	9
Figure 2.4 Covalent bonds in methane using electron line diagram.	10
Figure 2.5 Energy diagram for Carbon.	10
Figure 2.6 Promotion of electron in the second group of orbitals.	11
Figure 2.7 Formation of a methane molecular orbital from a carbon atom and four hydrogen atoms.	12
Figure 2.8 The covalent bond in ethylene using electron line diagram.	12
Figure 2.9 The shape of orbitals in the second group of a carbon after hybridization to form ethylene.	13
Figure 2.10 Sigma bond in ethylene molecule.	13
Figure 2.11 Pi bonds in ethylene molecule.	13
Figure 2.12 Covalent bonds in benzene using diagram.	14
Figure 2.13 Sigma bonds and pi bonds in benzene.	14
Figure 2.14 The field effect transistor and its operation principle.	16
Figure 2.15 The structure of an organic field effect transistor.	17
Figure 2.16 The band diagram of metal and p-type organic semiconductor contact.	18
Figure 2.17 The Band diagram of materials.	19

Figure 2.18 The surface plasmon resonance with the same frequency between surface electrons and incident light.	20
Figure 2.19 The w-k diagram.	21
Figure 2.20 The Kretschmann configuration.	21
Figure 2.21 The localized surface plasmon of metal nanoparticle.	22
Figure 2.22 The scattering as a function of wavelength for the different particle volumes.	23
Figure 2.23 The scattering of light by metal nanoparticle as a function of the wavelength depending on the refractive index of its surrounding materials.	23
Figure 3.1 The bottom gate structure with top drain and source electrodes of OFET for the experiment.	24
Figure 3.2 The structure of the wafer.	25
Figure 3.3 The electrode patterns for the organic field effect transistor; the channel width of electrodes: 1000 μm , 2000 μm , 3000 μm , and 5000 μm , the channel length: 10 μm , 20 μm , and 70 μm	25
Figure 3.4 The structure of the wafer with two gold electrodes.	26
Figure 3.5 Schematic band diagrams of the interfaces between P3HT and gold; (a) as-prepared P3HT, (b) thermally annealed P3HT.	27
Figure 3.6 The principle of absorption spectra measurement in organic semiconductor.	27
Figure 3.7 The absorption spectra measurement using a spectrometer and a halogen lamp.	28
Figure 3.8 The operating principle of grating.	28
Figure 3.9 Halogen lamp spectrum as light source.	29

Figure 3.10 The absorption spectrum of P3HT.	29
Figure 3.11 The principle of spectral response measurement in organic semiconductor.	30
Figure 3.12 The process of the spectral response measurement by using lock-in amplifier and optical chopper.	31
Figure 3.13 Voltage value for spectral response of the OFET.	32
Figure 3.14 The current value for spectral response of the OFET.	32
Figure 3.15 The power for each monochromatic light measured with its wavelength from the halogen lamp.	33
Figure 3.16 The spectral response curve of the OFET.	33
Figure 3.17 The current-voltage characteristic curve of the OFET.	34
Figure 3.18 The process of the current-voltage characteristic curve measurement.	35
Figure 3.19 Current–voltage characteristic curve of a P3HT OFET at different gate voltages.	35
Figure 4.1 From meter scale to nanoscale materials.	37
Figure 4.2 The distribution of surface atoms according to the size of gold nanoparticles.	38
Figure 4.3 The colloidal gold nano rods with absorption spectra peak at 710nm wavelength.	39
Figure 4.4 The deposition of Gold Nano Rods.	40
Figure 4.5 The deposition of gold nanoparticles by vacuum evaporation.	40
Figure 4.6 The absorption spectra of the gold nanoparticles assembled from 2nm thick film coated on a transparent glass by an evaporator.	41

Figure 4.7 The absorption spectra depending on the diameter of the colloidal gold nanoparticles.	42
Figure 5.1 The spectral response curve of the OFET at Gate Voltage: 5V, leakage: 0.00117 μ A, Drain-Source Voltage: 5V and Drain-Source Current: 0.19 μ A.	43
Figure 5.2 Voltage value for spectral response of the organic field effect transistor deposited with gold nanoparticles.	44
Figure 5.3 The current value for spectral response of the organic field effect transistor deposited with gold nanoparticles.	45
Figure 5.4 The spectral response curve of the organic field effect transistor deposited with gold nanoparticles at Gate Voltage: 5V, Drain-Source Voltage/Current: 5V/0.73 μ A.	45
Figure 5.5 The spectral response curve of the organic field effect transistor deposited with gold nanoparticles at Gate Voltage: 5V, Drain-Source Voltage: 1V and Drain-Source Current: 0.13 μ A.	46
Figure 5.6 The spectral responses at 5V gate voltage without gold nanoparticles and at 5V and 1V gate voltage with gold nanoparticles.	47
Figure 5.7 The difference of the normalized spectral response between the OFETs with gold nanoparticles and without gold nanoparticles.	47
Figure 5.8 The process of charge transfer at 550~650nm wavelength.	48
Figure 5.9 The process of charge transfer below 550nm wavelength.	48
Figure 5.10 The enhanced drain-source current of the OFET up to 3.84 times with gold nanoparticles at 5V gate voltage and 5V drain-source voltage.	50
Figure 6.1 The normalized spectral response of the OFET with and without Au NP. ...	51

Chapter 1: Introduction

Transistors operate same as vacuum tubes, but are smaller, cheaper, require less power, and obtain faster switching times. This small device makes alternating current to direct current. It receives and filters out radio waves. The received radio wave is converted into amplified sound and image. Currently, no one can deny the fact that this small device has developed the computer, radio, television and consumer products and has brought about technological innovation.

Transistor was invented for the first time by William Shockley, John Bardeen, and Walter Brattain at Bell Labs in 1947. The invention of the transistor was the result of efforts to create an amplifier by using semiconductor crystals instead of a vacuum tube. The amplification phenomenon was observed in the structure of two erected metal needles very close to the surface of the germanium crystal. In 1948, Shockley completely interpreted the amplification phenomena using the theory of p-n junction. The ideal form of junction transistor was invented. Shockley's transistor was the transistor based on the principle of the current flowing through crystal. It was quite different from the theory of Bardeen and Brattain that electrons moved in the surface a semiconductor crystal.

Shockley has made a field effect transistor by another principle in 1952. Because of this, the two strains, unipolar transistor (field effect transistor) and bipolar transistor (bipolar junction transistor) were presented as an active semiconductor components. Typically a transistor consists of semiconductor component with three terminals to connect an external circuit. Voltage (field effect transistor) or current (bipolar junction transistor) applied to one pair of the terminals controls the current through another pair of terminals. The three men were awarded the Nobel Prize in 1956. Field effect transistor

was completed as metal oxide semiconductor field effect transistor (MOSFET) in the 1960s. MOSFET is being used to create a number of great products.

Transistor may be used for switch or amplifier. It is also suitable to achieve the miniaturization of the device. In addition, low-cost production is possible due to its low temperature properties. MOSFET has all the necessary elements as a standard component of integrated circuits used in modern computers. FET is commonly used for weak-signal amplification. The active material's resistance between drain and source electrodes is controlled by a gate voltage. Thus, the current of FET can be modulated by using small voltage. This is originated from the contribution of its electrical properties as a transistor operation.

It also has optical detection properties as a field effect transistor based detector. A common type of a light-sensitive transistor is called a phototransistor. The phototransistor is a semiconductor light sensor formed from a basic transistor with a transparent cover. It was invented by Dr. John N. Shive (more famous for his wave machine) at Bell Labs in 1948. [1] However, it wasn't announced until 1950. [2] The electrons generated by photons are transferred to the drain, and the drain-source current is amplified by the gate voltage.

Another kind of field effect transistor is thin film transistor (TFT). In the MOSFET, the substrate and the active material are identical. However, in the TFT the active material, the other components of the FET, are deposited on a substrate in form of thin film. The TFT used CdSe as semiconductor active material was released for the solid-state image sensing device in 1949. In 1973, the examples applied to liquid crystal display (LCD) were presented. Use of the silicon in the semiconductor is in form of

amorphous and polycrystalline films. The amorphous films were developed at the University of Dundee in the UK in 1979 and the liquid crystal display applications were researched and developed mainly in Japan. TFT of amorphous silicon and polycrystalline silicon has been widely applied to a color TFT-LCD.

From the late 1970s, it is known that certain organic material through a suitable doping can be reached nearly close to the electrical conductivity of copper. [3] So far, all parts of the material from the top insulator (polystyrene) to the best superconductor ((TMTSF) 2PF_6 , perchlorate etc.) including a semiconductor and a conductor (doped polyacetylene) were able to be obtained by using organics.

In addition, the study about the use of organic semiconductor, organic field effect transistor (OFET), instead of the inorganic semiconductor in the active layer of the thin-film transistor was started since 1980. [4] OFET can be useful in case of the device fabricated over a large area, the need for a low temperature process, the bendable device, and in particular the low-cost process. The researchers in Philips surprised the world when they produced programmable code generator with 326 transistors by only using the polymer substrate, electrode, insulator, and semiconductor. [5]

The organic materials with semiconductor properties have been developed and applied to various categories over recent years. The area of the applied research using organic semiconductor, such as the organic light emitting diodes (OLED) displays, organic thin film transistors (OFET), solar cells, organic semiconductor memory devices using the multi-photon absorption phenomenon, continues expanding. [6] However, the most of the researches are limited to the organic light emitting diode. Although various

possibilities are open to this area, it has been studied only in a limited portion due to process complexity and cost issues. [7]

Especially, OLED displays in this field has already been commercialized and played important roles in activating the applied research using organics. Beginning with the active circuit for driving an OLED, organic field effect transistors, which are also expected as the next-generation smart card applications, are making a meteoric rise.

The organic semiconductor transistor can be produced in the same processing conditions of OLED such as organic semiconductor deposition method because the organic material for the OFET is same as the organic semiconductor of OLED in the nature of the material and physical and chemical properties are similar to each other. In addition, because both of them can be processed at room and low temperatures (less than 100 degrees Celsius), it is possible to manufacture an organic electroluminescence device based on plastic using the organic transistor. In the same vein, OFET can be used to implement the bendable liquid crystal display device based on the plastic substrate.

Transistors using organic materials, unlike the traditional silicon-based transistors, are small size, lightweight, and simple for fabrication. Therefore, it is in the spotlight as the next generation transistor to be applied to the future display. One of the advantages of the organic materials is its tunable electrical and optical properties. By changing its molecular structure or modified elements, the organic materials can be easily changed their material properties. However, the organic transistor has a characteristic of the low charge mobility compared with silicon and germanium. Thus, it cannot be used in the device that requires a high speed. In other words, low carrier mobility is a critical hurdle

to develop high performance device operation. Its low mobility limits the operation speed of the device, efficient amplification and carrier transport in a detector device.

The aim of this thesis is to increase the optical and electrical properties of organic field effect transistors by using metal nanostructure. Typically, metals such as gold and silver have abundant free electrons that can possibly increase conductivity of the device. In addition, a fascinating nanophotonics property, called surface plasmon resonance, can enable tunable optical response from visible to IR spectral range. [8] Therefore, the emergence of metal nanostructure has realized the enhanced optical and electrical properties of the organic materials that are applied to organic field effect transistors, organic light-emitting diodes, and organic photo-voltaic cells. [6] In this thesis, we have incorporated metal nanostructure into an organic semiconductor based device to increase its conductivity and to tailor its optical response.

Therefore, in chapter 2 the fundamentals of organic semiconductor, organic field effect transistor and surface plasmon resonance will be introduced. In the literature, surface plasmon resonance (SPR) has been studied by many scientists because various disciplines are related with it. [9] SPR presents the solution to deal with electromagnetic waves including light. [10] Particularly, optical properties of the luminescence such as fluorescence and phosphorescence can be obtained with improved efficiency by the surface plasmon resonance. [11] Metal nanoparticles contribute the intensity of light-emitting diodes to be enhanced by absorbing light and transferring energy. [12] The enhanced optical properties of organic light-emitting diodes are being announced by applying the surface plasmon resonance. [13] The reason for these increased optical

properties is explained by free electrons and energy transfer from the metal surface to the organic material. [14]

In chapters 3 and 4 one approach to fabricate gold nanoparticle incorporated in organic transistor is presented. Poly[3-hexylthiophene-2,5-diyl] (P3HT) as the active material in the organic transistor, was utilized. Organic semiconductor of the OFET, which is bottom gate with top drain and source electrodes, has been deposited by spin coating at room temperature. Metal nanoparticles have been deposited by vacuum evaporation of small molecules on the surface of the OFETs. Among metals, gold has excellent surface stability, thus gold has been used in this experiment. The spectral response and absorption spectra of OFET were measured to investigate the optical property. The electrical properties of the OFET have been measured by source meters. The absorption spectra of gold nanoparticles were measured in chapter 4.

The enhanced optical and electrical properties of the hybridization using polymer semiconducting materials and gold nanoparticles were observed and discussed in chapter 5. The last chapter deals with important consideration and future work about metal nanoparticles incorporated in organic field effect transistor.

Chapter 2: Background

In this thesis, we focus on enhanced optical and electrical properties for an organic transistor for a light detection application. The function of the organic semiconductor materials somewhat similar to the inorganic semiconductor materials, but there are significant difference in the working mechanism and basic properties. In this chapter, we will review basic optical and electrical properties of organic semiconductor materials. Also, we will review on surface plasmon resonance which is a proposed approach for tailored optical response and improved electrical properties for an organic thin film transistor.

Organic Semiconductor

Organic materials mainly consist of carbon, hydrogen and oxygen compounds. [15] Semiconductors have electrical conductivity properties between insulators and metals. Organic semiconductors mean the organic materials with semiconductor properties. The semiconductor properties of organic materials are originated by the special characteristic of pi electrons. Pi electrons are in the middle of free-electrons and bound-electrons. When single bond and double bond alternately appear between carbons, electrons are away from the nucleus. This enables the electrons to move easily by an applied electric field. Therefore, the polymer structure become conductive and flow currents when voltage is applied. [16]

In order to better understand the pi electron and organic semiconductor, orbital theory will be introduced. According to the orbital theory, the probability that electrons will be found can be only known in certain 3-dimensional space. [16] The orbital is a mathematical function of the probability. Orbitals are divided into several types such as s-orbital, p-orbital, and d-orbital according to the shape of the orbital as shown in Figure

2.1. These orbitals can be broken down into several types in accordance with three-dimensional structure, with the exception of spherical-shaped s-orbital. For example, p-orbital is dumbbell-shaped, being centered on the nucleus which is separated into p_x , p_y , p_z with subscripts x, y and z depending on the symmetrical axis of rotation in three-dimensional space as shown in Figure 2.1 (b)

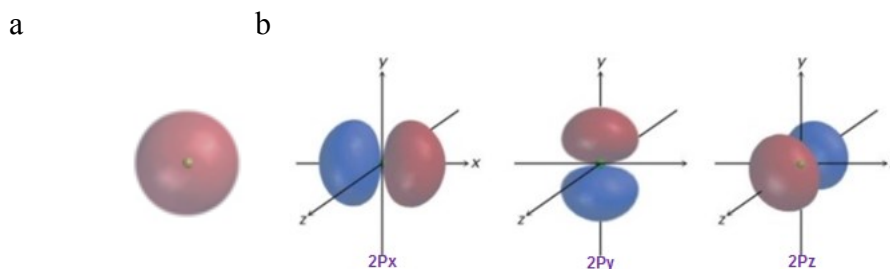


Figure 2.1 The shapes of orbitals depending on the symmetrical axis of rotation in three-dimensional space. (a), s orbital. (b), p_x orbital, p_y orbital and p_z orbital. [15]

Arranged in order in accordance with energy levels of electrons contained within orbitals, the orbitals which have similar energy levels can be found. These orbitals are in a group and a number can be given in front of each name. For example, the lowest energy level group, which is the first group, has only one s-orbital. The s-orbital can be named as 1s with the number one prefixed. In the following group, there are a total of four types of orbitals, s, p_x , p_y and p_z . They have a number 2 in front of the tags. That can be named as 2s, $2p_x$, $2p_y$ and $2p_z$ as shown in Figure 2.2.

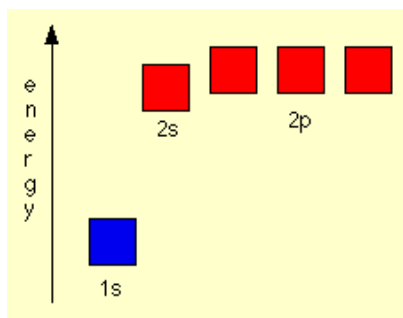


Figure 2.2 Energy diagram for 1s, 2s, $2p_x$, $2p_y$ and $2p_z$ orbitals. [17]

Each orbital can contain up to two electrons. The number of electrons contained within an orbital does not change its appearance. The outermost of these atomic orbitals are combined into a single molecular orbital to form a covalent bond. The shared electron pair is then free to move the entire giant molecular orbitals.

There are two kinds of method to form a molecular orbital. First, sigma bond (σ bond) mechanism is a method in which atomic orbitals are directly put together to form a giant molecular orbital as shown in Figure 2.3.

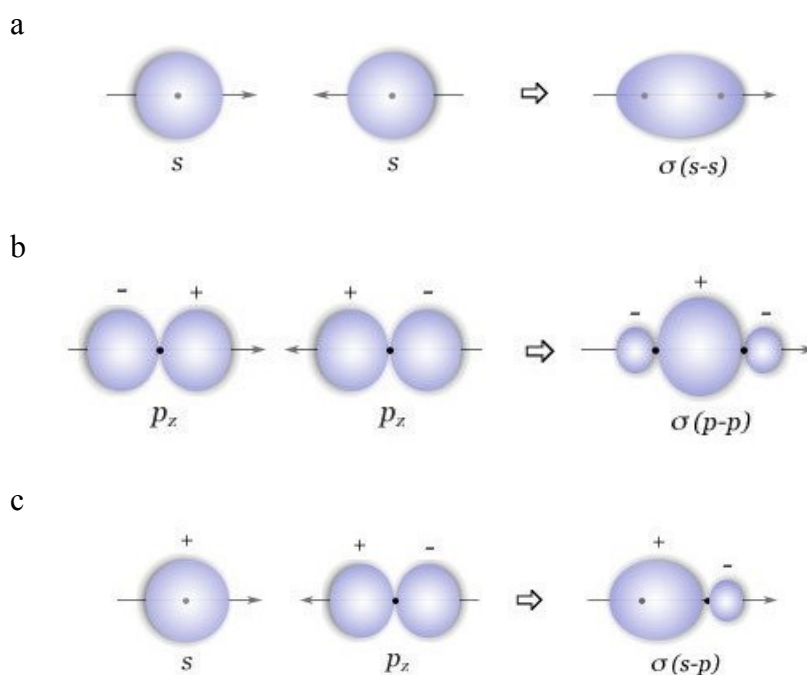


Figure 2.3 Formation of a Sigma bond. (a), A covalent bond resulting from the $\sigma(s-s)$ formation of a molecular orbital by the end-to-end overlap of s type atomic orbitals. (b), A covalent bond resulting from the $\sigma(p-p)$ formation of a molecular orbital by the end-to-end overlap of p type atomic orbitals. (c), A covalent bond resulting from the $\sigma(s-p)$ formation of a molecular orbital by the end-to-end overlap of s and p type orbitals. [17]

In the case of many atoms which are combined together such as methane (CH_4), one

carbon atom and four hydrogen atoms form four single covalent bonds. The appearance of a single covalent bond is chemically completely identical as shown in the Figure 2.4.

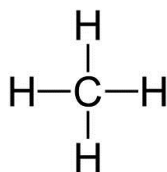


Figure 2.4 Covalent bonds in methane using electron line diagram.

However, the state of the atomic orbital of carbon is as shown in the Figure 2.5.

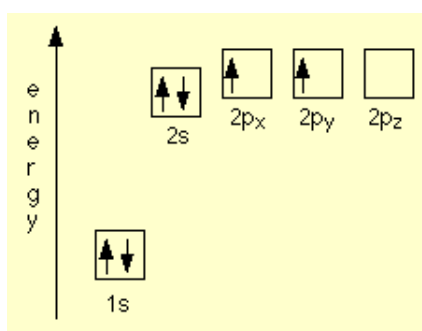


Figure 2.5 Energy diagram for Carbon. [17]

In fact, the only three existing outermost orbitals are 2s, 2p_x and 2p_y. These orbitals are not consistent with the Figure 2.4. Furthermore, it seems that only 2p_x and 2p_y can be combined with other orbitals because 2s orbital already has two electrons. This means that at best, only two can be combined with hydrogen. Because of this, one electron of the 2s orbital is excited receiving energy to go to 2p_z. This process is called promotion of electron. The electron is translated from the ground state to the excited state. Atoms are not covalently bonded because they exist around each other at the same time; rather, atoms are covalently bonded when constant energy is applied to the two materials. Promotion of electron occurs due to the energy that allows both atoms to bond.

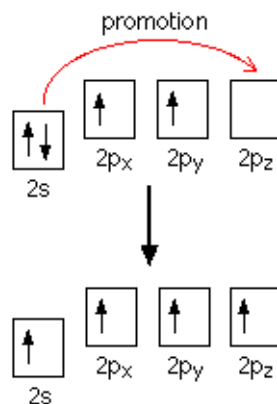


Figure 2.6 Promotion of electron in the second group of orbitals. [17]

But the problem still remains. As shown in Figure 2.6, the 2s orbital with only one electron is completely different in shape from other orbitals in the second group. Thus, four covalent bonds cannot be made in exactly the same shape. After that, four atomic orbitals in the second group become completely four new atomic orbitals with the same shape impacting to one another. Then, they can make the same shape of four covalent bonds. This series of the process is called hybridization.

The new atomic orbitals made from the orbitals in the second group are called hybrid orbitals. The hybrid orbitals are also classified into several types, according to kind of orbitals and number of orbitals. One s-orbital and one p-orbital make two sp hybrid orbitals. One s-orbital and two p-orbitals become three sp² hybrid orbitals. One s-orbital and three p-orbitals form four sp³ hybrid orbitals. For example, before methane molecules are formed, four sp³ hybrid orbitals are generated in the shape of a chicken leg as shown in the Figure 2.7. Then, these four hybrid orbitals meet s-orbitals of hydrogen respectively to form the following four molecular orbitals.

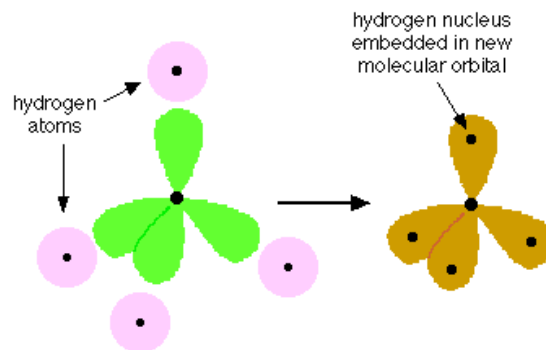


Figure 2.7 Formation of a methane molecular orbital from a carbon atom and four hydrogen atoms. [17]

Second, pi bond (π bond) mechanism is the method in which orbitals are not directly combined, but electrons can move between orbitals in the combined method. It is unlikely to find electrons in the middle of the space between p-orbitals. The pi bond can be found only in multiple covalent bonds such as ethylene (C_2H_4).

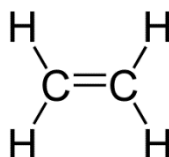


Figure 2.8 The covalent bond in ethylene using electron line diagram.

Ethylene has two carbon atoms in the center, and a double bond occurs between them as shown in Figure 2.8. Each of the two carbons has a single bond with two hydrogens in the side branches. The double bond in the middle has one sigma bond and one pi bond. From the perspective of each carbon, the carbon needs three hybrid orbitals because carbon combines with the three surrounding materials, one carbon and two hydrogens. The problem is that the second group of a carbon has four orbitals. Only three of them can become hybridized. Hence, because hybridization is not conducted for a single orbital, eventually this p-orbital keeps such shape as shown in the Figure 2.9.

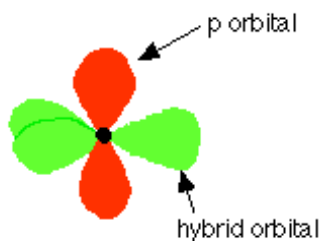


Figure 2.9 The shape of orbitals in the second group of a carbon after hybridization to form ethylene. [17]

After forming the shape, the carbon combines with surrounding two hydrogens and one carbon which makes sigma bond three times as shown in the Figure 2.10.

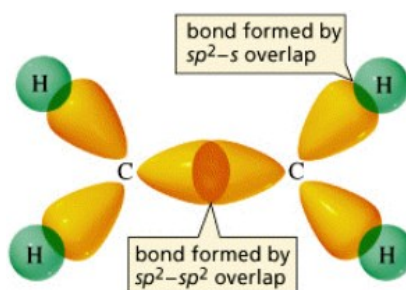


Figure 2.10 Sigma bond in ethylene molecule. [18]

Two vertically extending p-orbitals from each do not participate in sigma bonds. They make a pi bond in the empty space as shown in the Figure 2.11.

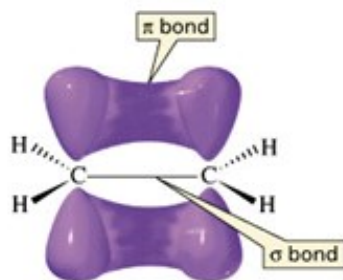


Figure 2.11 Pi bonds in ethylene molecule. [16]

Strictly speaking, the two orbitals retain the existing shape as before the pi bond. Because of this, they do not overlap each other. Electron may jump out of its own orbital region toward other orbital area, which is called delocalization of electron. [19]

Benzene conducts more complex double bond. Benzene has six carbon ring structure, and each of them has hydrogen in the side as shown in Figure 2.12.

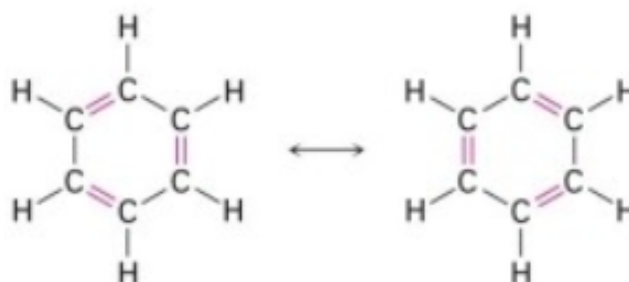


Figure 2.12 Covalent bonds in benzene using diagram.

The biggest feature of the benzene is to appear a double bond and a single bond in the center of carbon ring repeatedly. It is called conjugated double covalent bond. The Figure 2.13 lists a sigma bond and pi bond in order. [20]

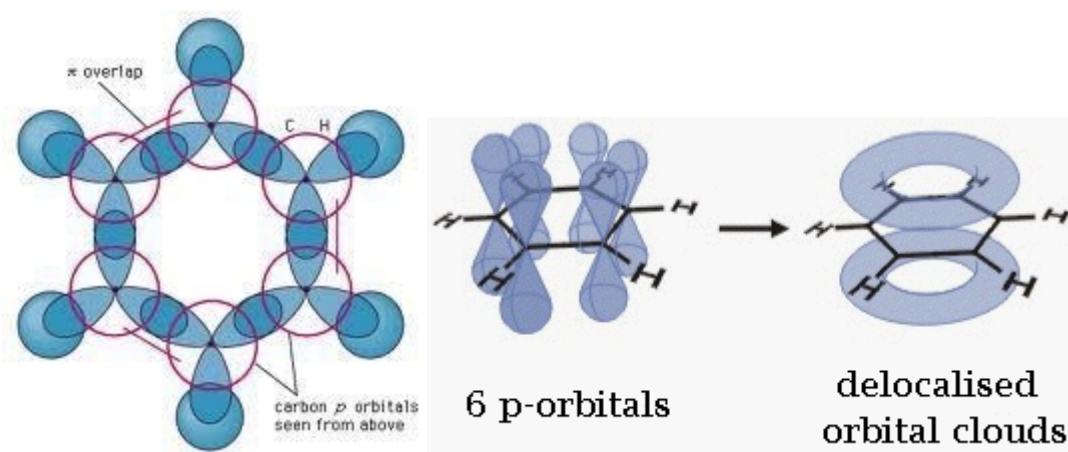


Figure 2.13 Sigma bonds and pi bonds in benzene. [17]

As can be seen from the right side of the Figure 2.13, the range of pi bonds is very broad. Originally, pi bond is supposed to be generated only in double bond areas. But benzene, which has conjugated double covalent bond repeatedly, can produce pi bond in a single bond existing between double bonds. This means that shared electrons are delocalized and can move in much wider area. This is because of resonance. Originally, the term comes from physics. As two substances vibrate with the same wavelength, they are amplified. This phenomenon also appears in chemistry.

In case of benzene, pi electrons in three double covalent bonds cause resonance to create significant vibration. So, the electrons can move around a single covalent bond. Moreover, as the pi electrons pass around the original single bond area, the single bond seems to become pi bond and double covalent bond. Each covalent bond becomes a double covalent bond and a single covalent bond repeatedly at incredibly fast speed within the hexagon area.

In the compound which has repeated conjugation, pi bond area can be more widened as compared with sigma bond area. After all the electrons in the pi bond are very liberal and can easily move out of the molecule when they get a little energy. In other words the pi electron is delocalized in the repeated conjugation. Organic semiconductor is made of conjugated molecules. [21]

Charges in organic semiconductors can flow by hopping of delocalized pi electrons between pi bonds. The formation of pi orbitals can explain the potential energy level of organic materials. The highest occupied molecular orbital (HOMO) refers to the orbitals at the highest point among orbitals which are filled with electrons in molecular orbital diagram. And the lowest unoccupied molecular orbital (LUMO) refers to the orbitals at

the lowest point among orbitals which are not filled with electrons. The optical and electrical properties of organic semiconductors are determined by the HOMO and LUMO levels. The more the number of conjugation of organic materials, the smaller the energy gap between LUMO and HOMO. When the difference between HOMO and LUMO energy levels gets fewer, electrons are likely to deviate. That means the organic materials can absorb a long wavelength such as visible light. [22]

Organic Field Effect Transistor (OFET)

A field-effect transistor (FET) is a type of transistor commonly used for weak-signal amplification. FET can control large current by using small gate voltage as shown in Figure 2.14. There are two kinds of field effect transistors. One is metal oxide semiconductor field effect transistor. The other is thin film field effect transistor. MOSFET is used for microprocessors and memory chips. TFT is suitable for non-Si material such as organic material.

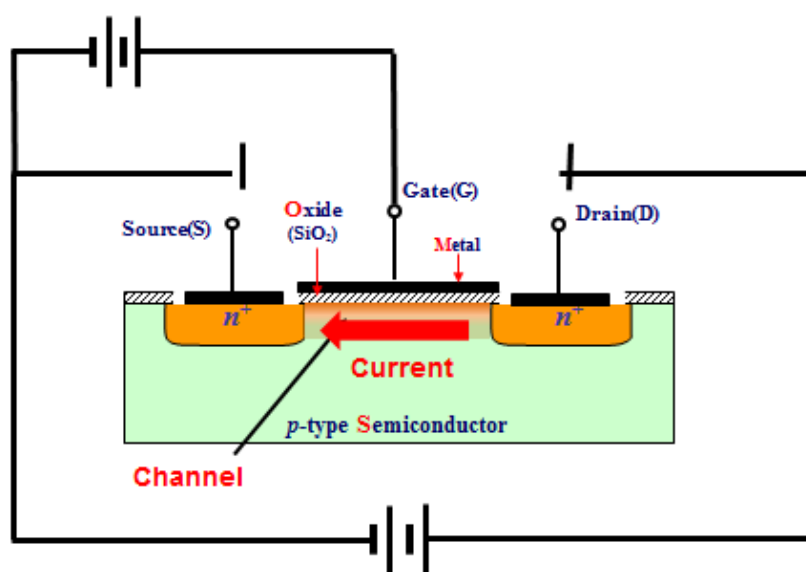


Figure 2.14 The field effect transistor and its operation principle.

The field effect transistors using organic materials are referred to organic field effect transistors like the Figure 2.15. Applying a voltage to the gate of the transistor, charges in the organic materials are pulled toward the gate. However, the insulator between the organic materials and the gate prevents the charges from being delivered to the gate. Those charges are gathered a lot over the insulator, the gathered charges form a channel, in which electrons generated in the source electrode can flow easily to the drain electrode. As gate voltage is increased, the channel is formed better and the drain-source current flows better.

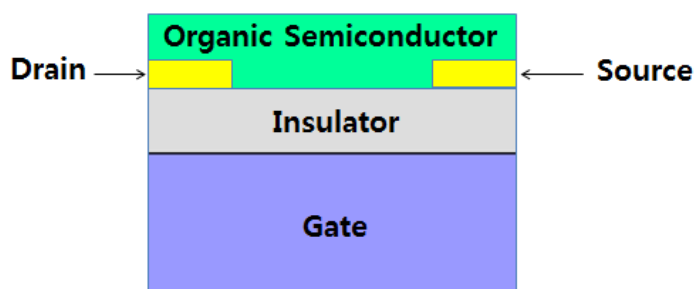


Figure 2.15 The structure of an organic field effect transistor.

The operation principle of the device reviewed with the concept of p-type semiconductors is that all the charge in the organic semiconductor spread evenly when voltage is not applied to source, drain and gate. At this time, voltage is applied between the source and the drain, current, which is proportional to voltage, flows. If positive voltage is applied to the gate, holes are pushed up because of the electric field. Hence, the holes are reduced close to the insulator. In this situation, the current flowing between the source and the drain is also reduced.

Conversely, positive charges between the organic material and the insulator are derived as negative voltage is applied to the gate. And thus the amount of charge is

formed close to the insulator. This is called accumulation layer. As current was measured by applying voltage between the source and the drain, the more current is able to flow.

There is also an energy barrier between a metal and an organic semiconductor. It depends on the work function of the metal and the work function of the organic semiconductor. [23] The height of the energy barrier can be adjusted by choosing a metal with the work function compared with the HOMO and LUMO energy level of the organic material [24].

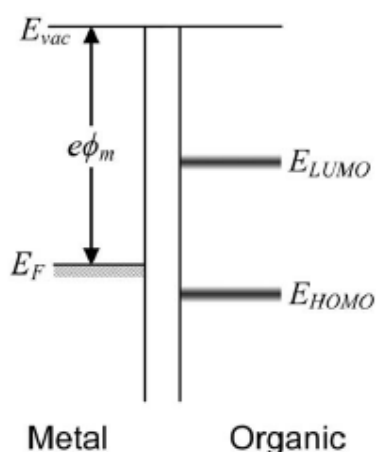


Figure 2.16 The band diagram of metal and p-type organic semiconductor contact. [25]

As shown in Figure 2.16, a small ohmic barrier is between the metal and the HOMO of the organic semiconductor, and a larger barrier exists between the metal and the LUMO of the organics. In this case, the organic semiconductor of the organic field effect transistor is kind of p-type material. [26].

Surface Plasmon Resonance (SPR)

Materials have band gap as shown in the Figure 2.17. The band gap is the energy difference between valence band and conduction band.

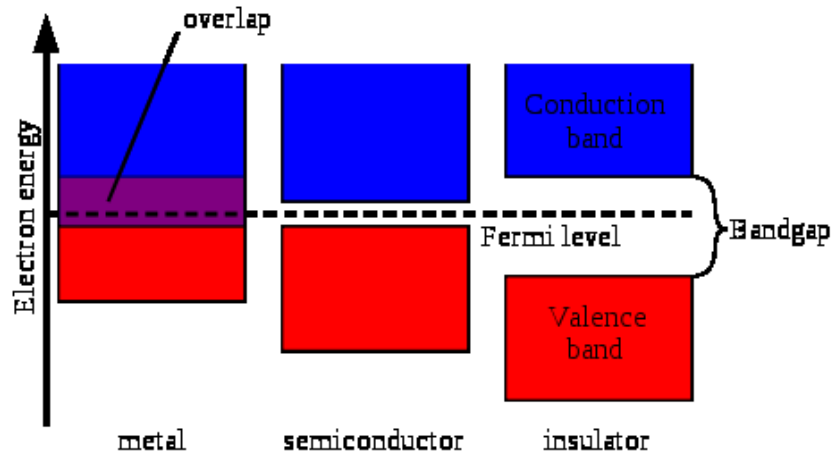


Figure 2.17 The Band diagram of materials.

The two bands are overlapped in metal diagram. Thus, metal is a conductor which has many free electrons in its conduction band. In other words, there are a lot of free electrons in the metal surface. [27]

The free electrons can be easily sensitized to specific external stimulus because they are not tied by the metal atoms. [28] These free electrons can vibrate on the metal surface with a certain wavelength and frequency under a particular condition. Plasmon is wave of charges on a metal and dielectric interface. This vibration of surface wave is called surface plasmon and typically it is observed from gold or silver. This surface plasmon refers to the collective oscillation of free electrons which is usually propagated along the interface between metal and dielectric. When the surface plasmon wave travels on the boundary between metal and dielectric material, the perpendicular field strength are exponentially decreased from the boundary. [29] In other words, the further the surface plasmon goes away from the interface between the metal and the dielectric, the further the surface plasmon decreases exponentially in a vertical direction. [30]

The oscillation frequency is determined by the dielectric constant of the metal and the dielectric. [31] The collective oscillation of the free electrons is increased by incident light from outside. As light energy is received by electrons, then the electrons are excited more and vibrate with large amplitude. [32] As the surface electrons with a certain frequency meet the light with the same frequency, the electrons is resonated and the amplitude of the vibrating electrons becomes the maximum as shown in Figure 2.18. This is referred to as surface plasmon resonance. [33] Surface plasmon resonance is transverse EM wave coupled to a plasmon.

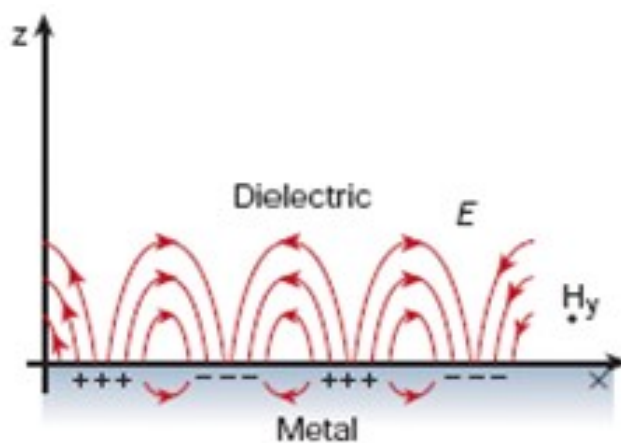


Figure 2.18 The surface plasmon resonance with the same frequency between surface electrons and incident light.

In order to excite SPR, the wave vector along with metal surface and dielectric surface should be matched. Typically, when the illuminate light comes from the dielectric side, the wave vectors between metal and dielectric cannot be matched as shown in Figure 2.19.

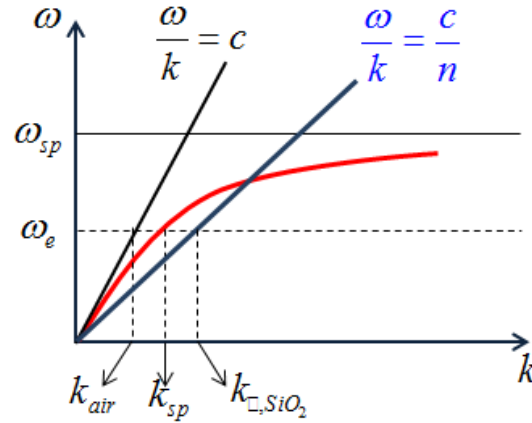


Figure 2.19 The w-k diagram.

In order to solve this problem, a prism can be attached on a metal surface as shown in Figure 2.20. This devised technique is called the method of Kretschmann configuration. Under this condition, the incident light from glass has larger wave vector than the wave vector on the metal surface that facing to air. Because a thin metal layer (typically $\sim 50\text{nm}$) is covered on the glass, the size of wave vector from glass can be maintained until it passes through the metal film. By changing the incident angle to the metal film through the glass, there should be a specific condition that makes the incident wave vector becomes same size of plasmon wave vector. If this occurs the incident electromagnetic wave energy can be strongly absorbed to create surface plasmon resonance.

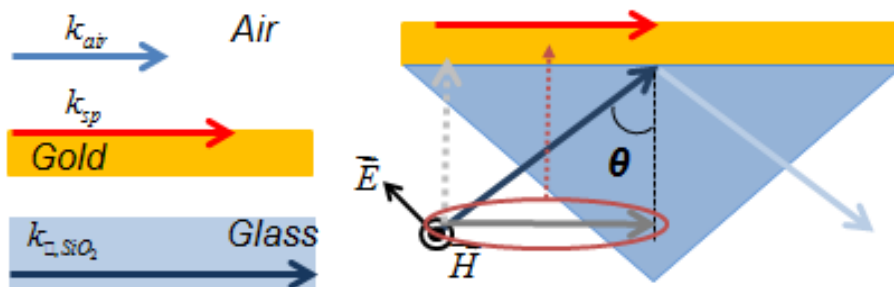


Figure 2.20 The Kretschmann configuration.

In particular, Transverse EM wave coupled to metal nanoparticles is called localized surface plasmon. [34]

Another plasmon effect can be observed in a 0 dimensional nanostructure. This is called ‘Localized Surface Plasmon Resonance’. Localized surface plasmon is not propagated in any direction but aggregated around the metal nanoparticles as shown in Figure 2.21. [31]

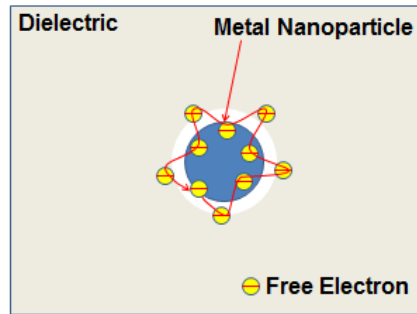


Figure 2.21 The localized surface plasmon of metal nanoparticle.

In case of metal nanoparticles, a sufficient level of the free electrons in the surface vibrates at a specific frequency, thus light with the specific frequency is strongly absorbed and scattered by the metal nanoparticles. [35] The metals which have this property are gold, silver, and copper. They release electrons easily by external stimulus and have negative dielectric constant. Among them, silver which has the sharpest surface plasmon resonance peak and gold which has excellent surface stability are mainly used. The metal nanoparticles are extremely strongly resonated in visible region of light. Scattering and absorption of light by spherical particles (very small particles compared with the wavelength of light) follow the equation as bellow (by Mie’s theory).

$$\sigma_{ext}(\lambda) = 18 \frac{\pi}{\lambda} \varepsilon_H'^{3/2} V_M \frac{\varepsilon_M'(\lambda)}{[\varepsilon_M'(\lambda) + 2\varepsilon_H']^2 + \varepsilon_M''(\lambda)^2} \quad (V_M: \text{particle volume})$$

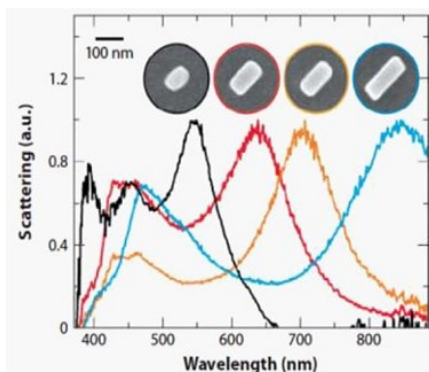


Figure 2.22 The scattering as a function of wavelength for the different particle volumes.

The scattering and absorption of light by metal nanoparticles are proportional to the volume of the metal nanoparticles as shown in Figure 2.22. Thus, the resonance wavelength or frequency of the metal nanoparticles can be changed by regulating the size and type of the nanoparticles, hereby suitable size and form of metal nanoparticles for desired wavelength range can be selected to obtain surface plasmon effect. [36]

In addition, the scattering and absorption of light by metal nanoparticles can be controlled by the refractive index of surrounding materials. As the refractive index increases, the wavelength of surface plasmon resonance related absorption shifts to longer wavelength as shown in Figure 2.23.

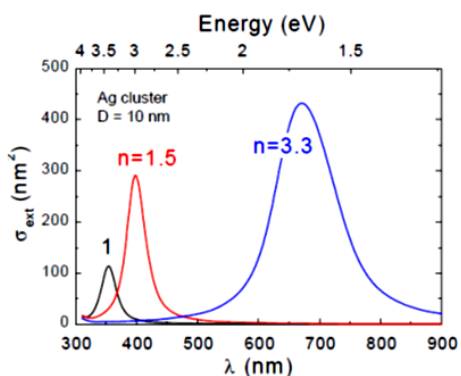


Figure 2.23 The scattering of light by metal nanoparticle as a function of the wavelength depending on the refractive index of its surrounding materials.

Chapter 3: FABRICATION and CHARACTERISTICS of OFET

In previous chapter, we have discussed about the background of organic semiconductor and surface plasmon resonance. Organic materials provide easy and low cost fabrication process and localized surface plasmon resonance (LSPR) in metal nanostructures can produce fascinating optical properties depending on its structural modifications. For the utilization of these properties and improved optical electrical properties, we will discuss about a prototype hybrid device using semiconducting polymer and metal plasmonic nanostructure. An all solution processed hybrid thin film transistor, consisting of an organic thin film transistor structure and self-assembled gold nanostructures that has plasmonic absorption in visible, was fabricated.

Fabrication of OFET

For the fabrication of OFET, two configurations are typically used; bottom gate configuration and top gate configuration. The bottom gate configuration is used in this experiment as shown in Figure 3.1.

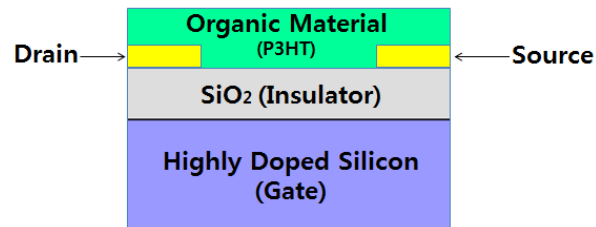


Figure 3.1 The bottom gate structure with top drain and source electrodes of OFET for the experiment.

For the bottom gate structure, as a gate, a highly doped silicon wafer has been used. Wafer was purchased from the University wafer and the initial Silicon wafer structure is shown in Figure 3.2.

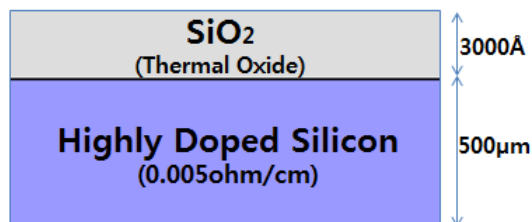


Figure 3.2 The structure of the wafer.

The thickness of the heavily doped silicon wafer is 500 micrometers. A thin layer of oxide (silicon dioxide) (300 nanometers thick) on top of the Silicon was produced as an insulator by thermal oxidation.

A mask for the electrode pattern was designed by commercial software (Layout Editor 2009) and the pattern was generated on a Cr coated glass photomask. Since the low mobility of the organic materials the device size was relatively larger than conventional solid state based thin film transistor. Various channel length and width for the thin film transistor was designed and the electrode patterns for the organic field effect transistor are presented in Figure 3.3

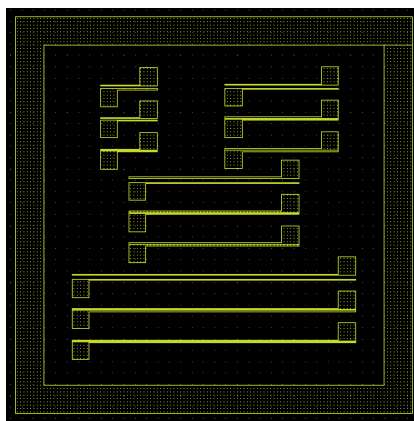


Figure 3.3 The electrode patterns for the organic field effect transistor; the channel width of electrodes: 1000μm, 2000μm, 3000μm, and 5000μm, the channel length: 10μm, 20μm, and 70μm.

Drain-source current is proportional to the channel width of electrodes and inversely proportional to the channel length between drain electrode and source electrode as bellow.

$$I_{DS} = \frac{WC_i}{2L} \mu (V_{GS} - V_T)^2 \quad (\mu = \text{mobility, } C = \text{capacitance})$$

The electrode pattern was transferred to a wafer by using a photo lithography process. Then gold film was deposited on the wafer to a thickness of 100 nanometers by evaporation in a vacuum chamber and a lift-off process was followed. The final structure after lift-off process is shown in Figure 3.4.

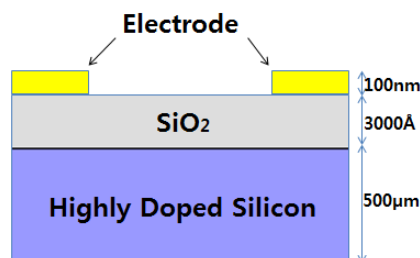


Figure 3.4 The structure of the wafer with two gold electrodes.

For an organic semiconducting material, P3HT (Poly(3-hexylthiophene-2,5-diyl)) was purchased from Sigma-Aldrich as an organic material. The P3HT has 5eV of the HOMO energy level and 3.1eV of the LUMO energy level. Thus, the energy difference between the HOMO and the LUMO is 1.9eV. The wavelength above which the P3HT cannot absorb the light is calculated by using equation $1.24/1.9\text{eV} = 0.652\mu\text{m} = 652\text{nm}$. The wavelength of the absorption spectra peak and the spectral response peak of the P3HT were 550nm. Organic material was spin-coated (1200rpm, 30sec) on the silicon wafer patterned with gold. After spin coating, the device was annealed at 150 °C for 10 minutes inside glove box to increase the charge mobility by crystallization of the organic semiconductor. The band diagrams of OFET are as shown in Figure 3.5.

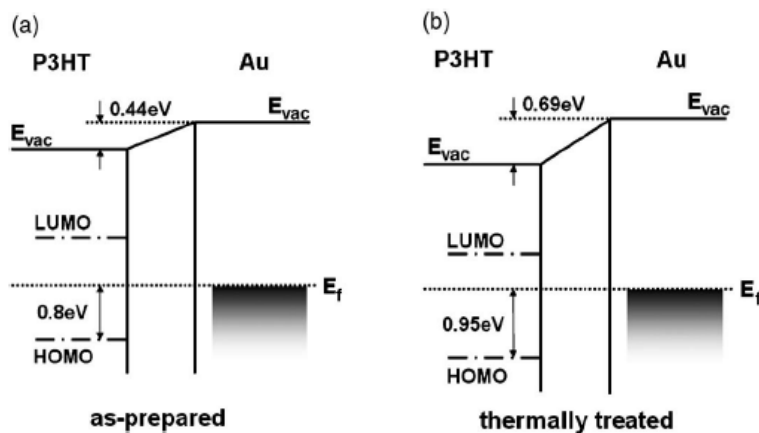


Figure 3.5 Schematic band diagrams of the interfaces between P3HT and gold; (a) as-prepared P3HT, (b) thermally annealed P3HT. [37]

Optical Properties of OFET

Optical properties are measured by spectral response and absorption spectra. A material's absorption spectrum is the fraction of incident radiation absorbed by the material over a range of wavelengths or frequencies. Organic semiconductors have many pi electrons. Pi electrons have energy between free electrons and bound electrons. They can be excited with a little energy to become free electrons. Even though the electron is excited in organic semiconductors, the electron is combined with a hole by coulomb attraction as shown in Figure 3.6. The free electron combined with the hole is called an exciton.

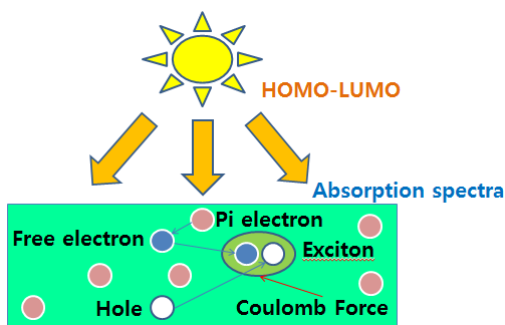


Figure 3.6 The principle of absorption spectra measurement in organic semiconductor.

As organic semiconductor receives energy greater than the energy difference between its HOMO and LUMO energy level, excitons are generated. The energy used to generate excitons is the same as the amount of light absorbed by the organic semiconductor. The result of measuring the amount of light is referred to as absorption spectra.

A BLACK-Comet UV-VIS spectrometer and a halogen lamp were used for the absorption spectra measurement. A spectrometer classifies light wavelength by using a 40mm diameter concave grating and measures the intensity of each wavelength. SpectroPro calculates and shows the absorption spectra as shown in Figure 3.7.



Figure 3.7 The absorption spectra measurement using a spectrometer and a halogen lamp.

The grating inside the spectrometer is used to produce spectral lines and the spectrometer measures their wavelengths and intensities as shown in Figure 3.8.

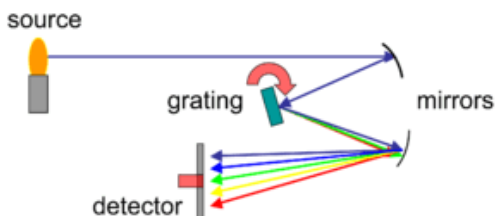


Figure 3.8 The operating principle of grating.

As one kind of incandescent lamps, a halogen lamp is the lamp to further suppress the vaporization of tungsten by injecting halogen materials in the glass sphere. The halogen lamp is brighter than incandescent bulbs and lasts longer. The halogen spectrum after

pass through a monochromator is obtained by recording the halogen light with a spectrometer as shown in Figure 3.9.

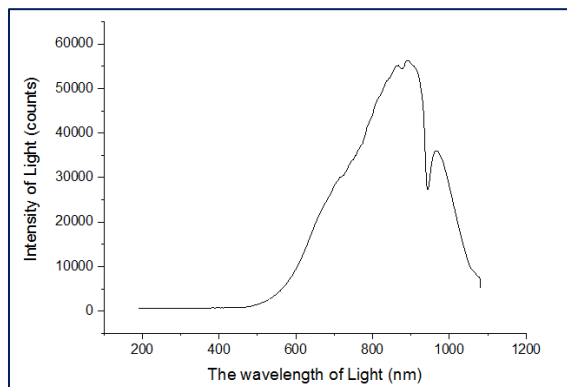


Figure 3.9 Halogen lamp spectrum as light source.

First, P3HT was spin coated on the surface of a glass. The absorption spectra of the organic material, P3HT, are gained by comparing the light passed through the glass before the spectrometer with the halogen lamp spectrum as shown in Figure 3.10.

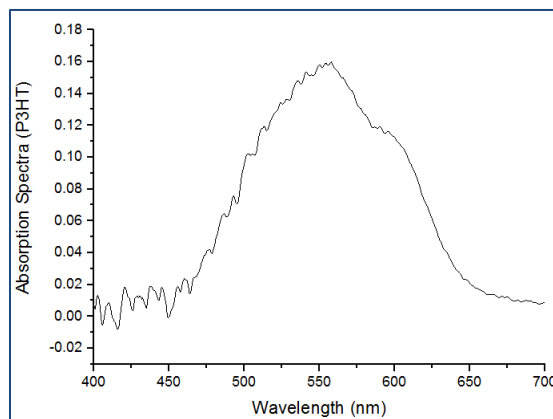


Figure 3.10 The absorption spectrum of P3HT.

The Difference of the energy level between the HOMO and the LUMO of P3HT is 1.9eV. The photon energy is inversely proportional to the wavelength of the light. Thus, the minimum wavelength of the light that P3HT can absorb is 652nm. The absorption

property of P3HT is consistent with the energy level gap of P3HT. The wavelength of the absorption spectra peak of the P3HT is 550nm.

Another optical property for OFET is spectral response. Spectral response, which is a function of wavelength, is the ratio of the current generated by a device to the power incident on the device. The process by which the exciton is generated in organic field effect transistors is the same as the process of the absorption spectra measurement. Excitons are separated by drain-source voltage of the organic field effect transistor as shown in Figure 3.11. The electrical field generated by the drain-source voltage should be bigger than the coulomb force of the exciton. As the drain-source voltage increases or the resistance of organic material decreases, the current generated by the excitons is increased more. Excitons are created in organic field effect transistors by light energy; the amount of current generated by the excitons is called spectral response.

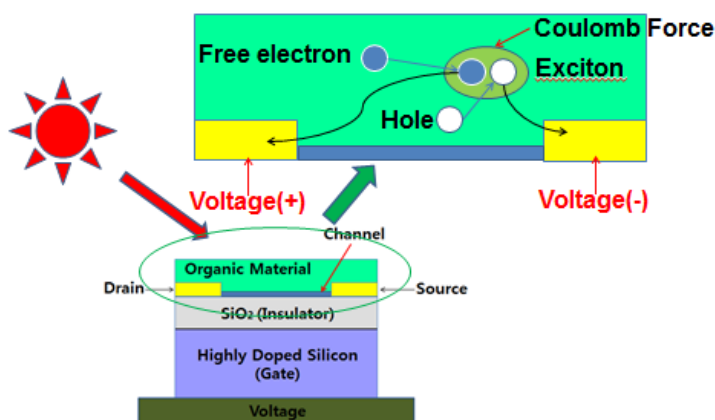


Figure 3.11 The principle of spectral response measurement in organic semiconductor.

Several instruments such as a SpectraPro 275 monochromator, SR540 Optical Chopper, a Micromanipulator probe station, two Keithley 2400 Source Meters, a halogen lamp, and a SR830 Lock-In Amplifier were used to measure the spectral response.

The measurement was carried out as following. First, a monochromator produces monochromatic light from a halogen lamp because the optical characteristic of a device is dependent on wavelength. Two source meters apply voltage to gate and drain-source of OFET respectively.

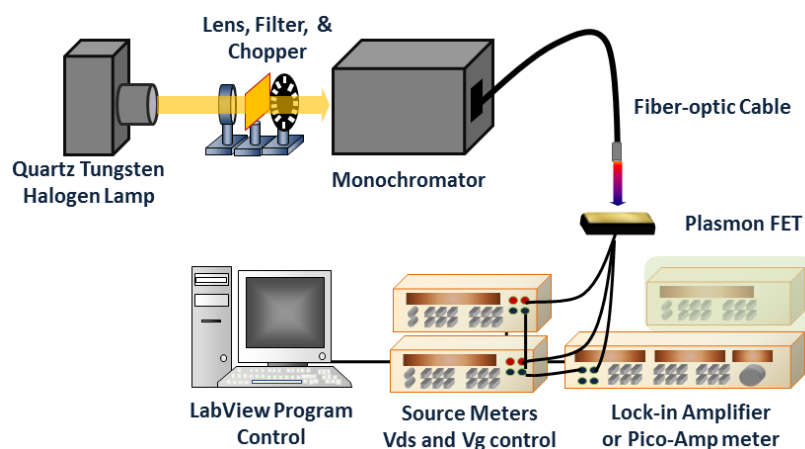


Figure 3.12 The process of the spectral response measurement by using lock-in amplifier and optical chopper.

In particular, the SR830 Lock-In Amplifier and SR540 Optical Chopper were used to detect and measure very small signals as shown in Figure 3.12. The operation principle of lock-in amplifier is known as phase sensitive detection technique to pick up the small signal obscured by very large noise. They make a reference frequency and reject noise with frequencies other than the reference frequency. Hence, noise signals do not affect the measurement. Since the device has a large voltage bias across Drain and source electrode, the drain current that was collected by the modulated light illumination was measured by an indirect method. We used a series resistor to a Drain-Source bias to produce the voltage value and it was converted to current value. The measured voltage value from the OFET is shown in Figure 3.13.

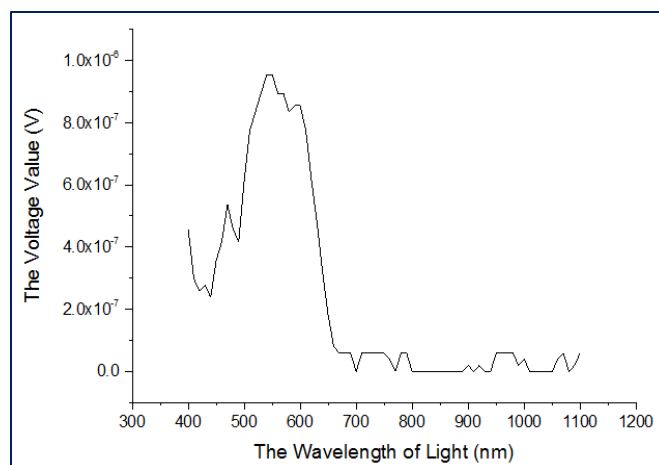


Figure 3.13 Voltage value for spectral response of the OFET.

To calculate the spectral response of the device the voltage value has to be converted to a current value. The voltage value is divided by the inserted resistor (65K ohm) and current value is obtained as shown in Figure 3.14.

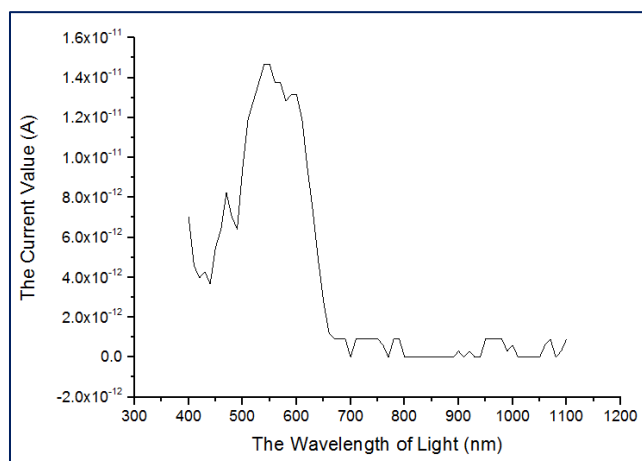


Figure 3.14 The current value for spectral response of the OFET.

A NIST calibrated reference photodetector was used to measure the actual power of the monochromatic light source. The reference spectral response of the reference solar cell was offered for the reference solar cell by the company. The voltage for each

monochromatic light was measured with its wavelength. The voltage was divided by the resistor and current value is obtained. Then, the reference spectral response was divided by the current and the power of monochromatic light for the halogen lamp was gained as shown in Figure 3.15.

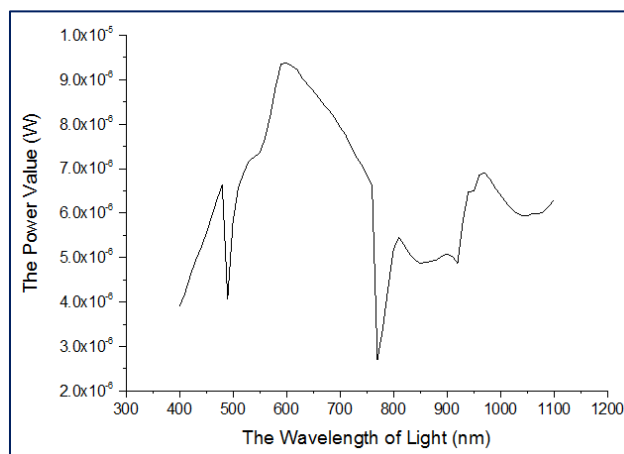


Figure 3.15 The power for each monochromatic light measured with its wavelength from the halogen lamp.

The current value of the OFET was divided by the power of the halogen lamp and the spectral response was obtained as shown in Figure 3.16. The wavelength of the spectral response peak of the P3HT was around 550nm.

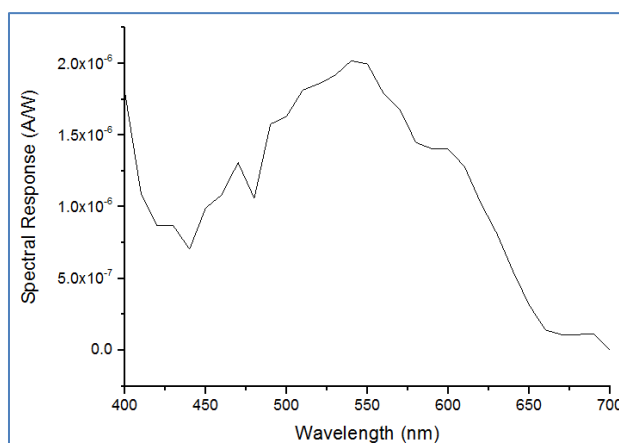


Figure 3.16 The spectral response curve of the OFET.

Electrical Properties of OFET

Figure 3.17 is current voltage characteristic curve of OFET. P3HT was used as an organic semiconductor. As gate voltage is increased, the channel is formed better and the current is increased. Since the P3HT polymer is p-type material, the majority carrier is a hole. Therefore the gate voltage needs to be controlled in negative valued to create a hole channel.

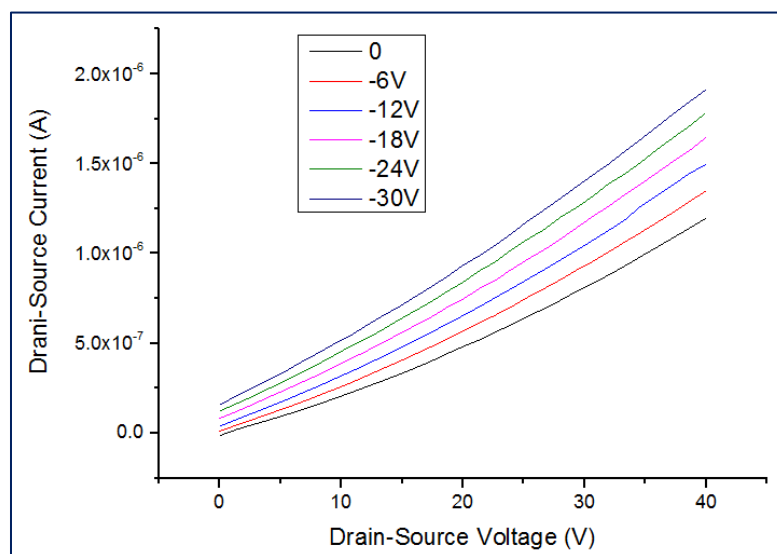


Figure 3.17 The current-voltage characteristic curve of the OFET.

The current-voltage characteristic curve was measured in a darkroom using two Keithley 2400 Source Meters and two probes on a Micromanipulator probe station. The OFET device is so tiny. Hence the device can be measured by using probes. Keithley 2400 Source Meter is an instrument to test tightly coupled sourcing and measurement. In other words, the source meter can act as voltage source and current source. At the same time, the source meter can act as voltage meter, current meter and ohm meter.

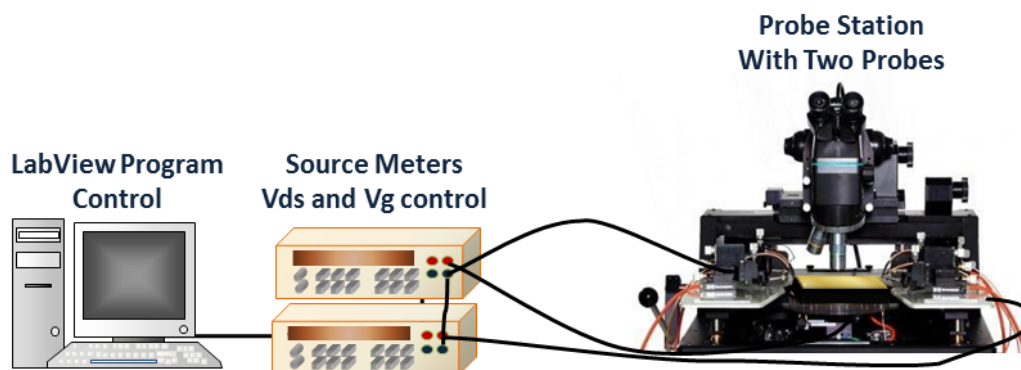


Figure 3.18 The process of the current-voltage characteristic curve measurement.

A source meter applied voltage to the gate and measured leakage current which passed through the insulator. The other source meter applied voltage to the drain-source and measured drain-source current. In order to measure accurately, delay time of the measurement and the voltage were applied automatically by a computer as shown in Figure 3.18. When the more voltage is applied to the gate, the channel is filled with holes, thus the current is easily transferred between the drain and the source.

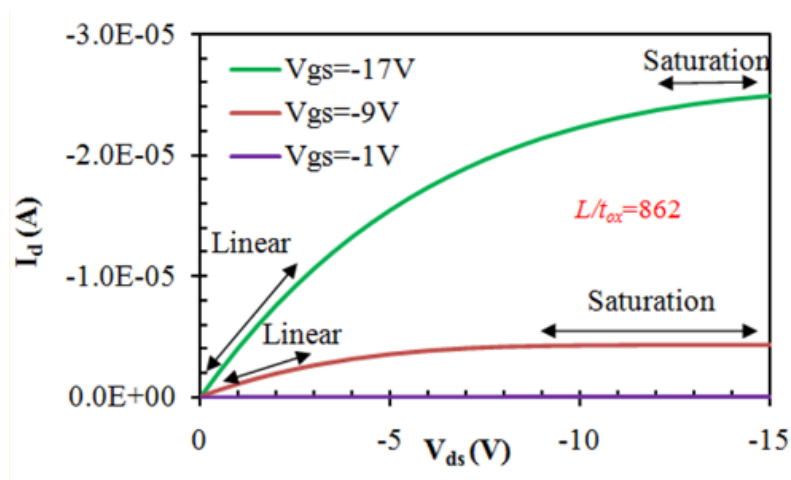


Figure 3.19 Current–voltage characteristic curve of a P3HT OFET at different gate voltages. [38]

Drain-source current is measured as a function of drain-source voltage at different gate voltage as shown in Figure 3.19. The drain-source current equation for linear region is as follows.

$$I_{DS} = \frac{W}{L} C_i \mu (V_{GS} - V_T) V_{DS} \quad V_{DS} \ll (V_{GS} - V_T); \text{ linear region} \quad [39]$$

The drain-source current equation for saturation region is as bellow.

$$I_{DS}^{\text{sat}} = \frac{W}{2L} C_i \mu (V_{GS} - V_T)^2 \quad V_{DS} > (V_{GS} - V_T); \text{ saturation regime} \quad [39]$$

In summary, an organic thin film transistor structure using P3HT conjugated polymer was successfully fabricated on a Silicon substrate. The electrical property was characterized and confirmed its p-type operation. In addition, we have observed transistor operation under weak positive gate bias which will be used for plasmon energy collection. The optical detection was available since the P3HT has an absorption in visible color. A lock-in measurement technique enabled the exact spectral response using drain current measurement under high voltage bias condition.

Chapter 4: OFET with METAL NANOPARTICLES

In this chapter, a nanoparticle incorporated hybrid organic transistor device will be discussed. In the beginning, a brief summary on metal nanoparticles and its plasmonic behavior will be summarized. Then, the hybridization methods using gold nanostructures and organic thin film transistors are discussed. We have successfully fabricated a gold nanoparticle incorporated organic transistor using thermal reflow method after a thin gold film deposition on the active region of the organic thin film transistor.

Metal Nanoparticles

Nano is a unit representing a billionth of a meter. One nanometer is one hundred thousandth of a hair thickness as shown in the Figure 4.1.

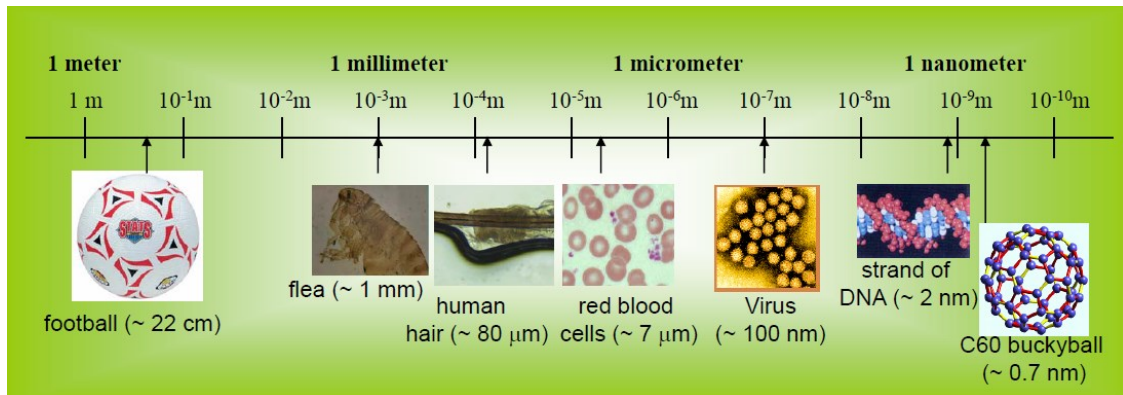


Figure 4.1 From meter scale to nanoscale materials.

Nano technology is the technique to control and identify the nature of substance to the nanometer level. In other words, nano technology can physically or chemically control substance at the level of atoms or molecules and fetch out the useful structures and functions of the substance. This technology makes it possible to build the device which has totally different principle from the previous one. Hence, it is expected to take advantage of limitless possibilities of nano technology.

In particular, size of metals is reduced to nanometer scale, the interesting phenomenon occurs. Metal nanoparticles, nano-scale metals, have totally different physical or chemical properties from conventional bulk metals. For example, the melting point is gradually going down in case the size of metal particles is smaller because surface area per unit volume increases if the size of the particles is smaller as below and thus the small particles of metals can absorb energy better than large particles of the same metals. [40]







Number of shell		Size	Total number of Atoms	Surface Atoms (%)
1 shell		6Å	13	92
2 shells		10Å	55	76
3 shells		14Å	147	63
4 shells		18Å	309	52
5 shells		22Å	561	45
7 shells		26Å	1415	35

Figure 4.2 The distribution of surface atoms according to the size of gold nanoparticles.

In other words, if the size of metal nanoparticles gets smaller, the proportion of surface atoms becomes larger. The energy of surface atoms is larger than the energy of internal atoms as shown in the Figure 4.2. Thus, when a metal has a large proportion of surface atoms with high energy, excellent chemical and physical reactivity of the nanomaterial appears. [36]

Among metals, gold has excellent surface stability, thus gold has been used in this experiment. Also, optical and electronic properties of gold nanoparticles are changed by

changing size and form of the particles. In particular, gold nanoparticles strongly interact with light depending on their size. [41] Oscillating electric fields of light passing through between gold nanoparticle and dielectric interact with the oscillating free electrons of gold nanoparticle at the same oscillating frequency between the light and the free electrons of gold nanoparticles causing a resonated oscillation of electron. This resonant oscillation is called surface plasmon resonance. Hence, light with the specific frequency is strongly absorbed depending on the resonance frequency of the oscillating free electrons of gold nanoparticles.

Fabrication of Gold Nanoparticles incorporated in Organic Transistor

Colloidal gold nanorods were used to check the change of the spectral response of the organic field effect transistor. The GNRs in an aqueous solution are produced as shown in Figure 4.3.

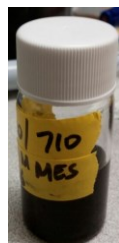


Figure 4.3 The colloidal gold nano rods with absorption spectra peak at 710nm wavelength.

The GNRs have absorption spectra peak at 710nm wavelength. The GNRs were coated on the organic field effect transistor in a variety of ways to make as shown in Figure 4.4, but failed. The GNRs are not coated on the surface of the organic material by drop casting and spin coating. Because its hydrophilic property, the GNRs are not mixed with the organic material.

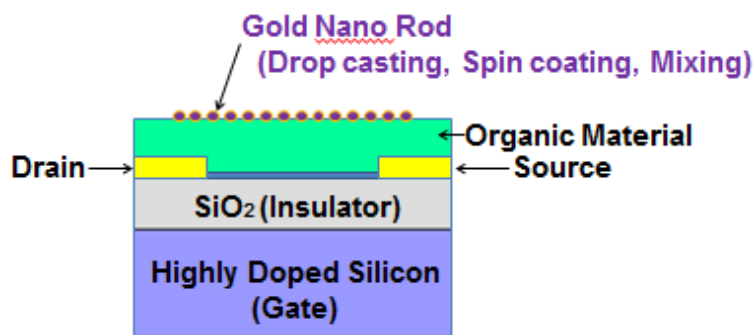


Figure 4.4 The deposition of Gold Nano Rods.

As an alternative approach, self-assembled gold nanoparticles are incorporated onto the organic active layer. To create this nanostructure, a thin gold film (2-6nm) was deposited by thermal evaporation on the surface of the OFET as shown in the Figure 4.5. Then the device was annealed at 150 °C for 10 minutes inside glove box to make the gold structures are melted and created a self-assembled structure.

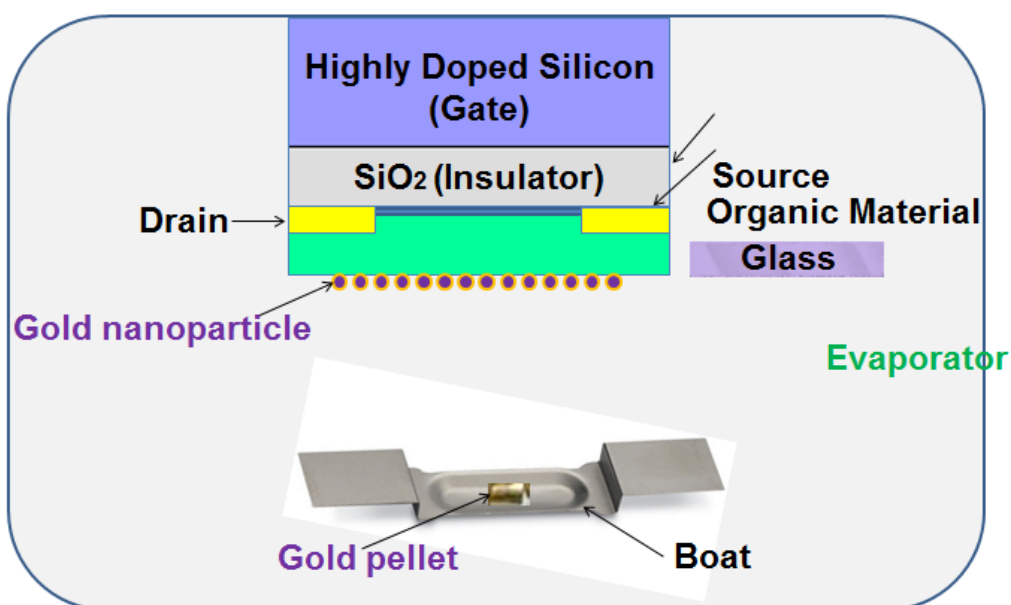


Figure 4.5 The deposition of gold nanoparticles by vacuum evaporation.

In order to check the optical properties of gold nanoparticles, an identical gold thin film was deposited on a transparent glass in an evaporator at the same time. Typical vacuum level was made around 3×10^{-6} torr and deposition rate was controlled between $0.1 \sim 0.5 \text{ \AA/s}$. Finally, the gold thin film was deposited to 2nm thickness on the glass then a post annealing process was followed to create self-assembled gold nanostructure. The absorption spectra of the gold nanoparticles on the glass are as shown in Figure 4.6.

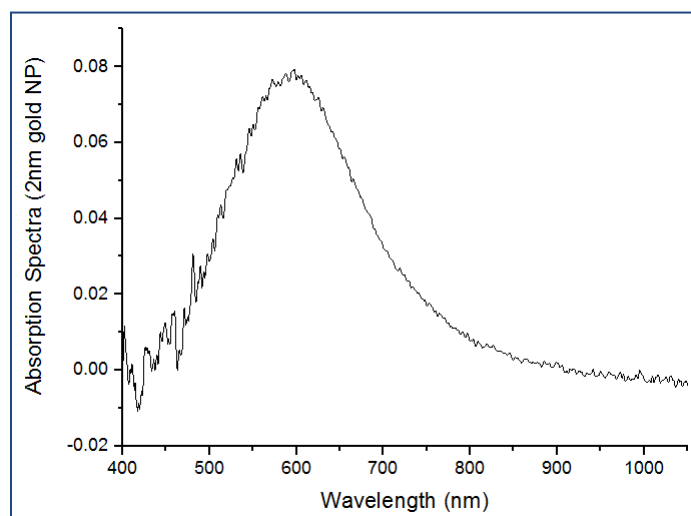


Figure 4.6 The absorption spectra of the gold nanoparticles assembled from 2nm thick film coated on a transparent glass by an evaporator.

From the gold nanoparticles assembled from 2nm thick film, the surface plasmon resonance phenomena cause light absorption around 600nm wavelength as shown in the Figure 4.6. But the size of the gold nanoparticles assembled from 2nm thick film is not 2nm in diameter. The 2nm gold nanoparticles should have the surface plasmon resonance peak below 520nm wavelength. As particle size decreases, the wavelength of surface plasmon resonance related absorption shifts to shorter wavelength as shown in Figure 4.7.

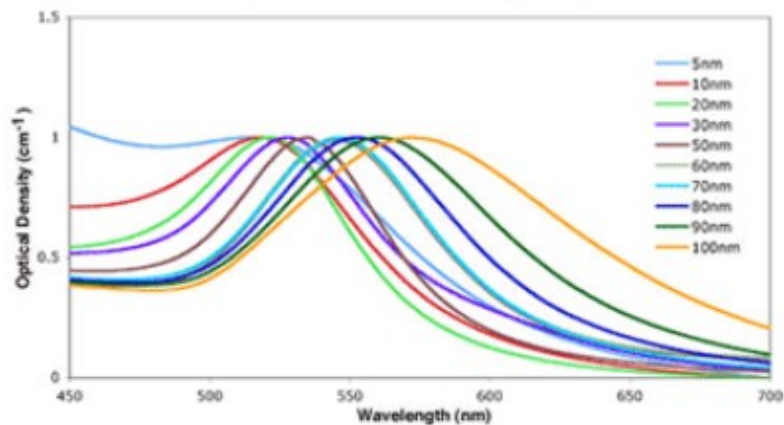


Figure 4.7 The absorption spectra depending on the diameter of the colloidal gold nanoparticles. [42] [43]

It can be assumed that the gold nanoparticles assembled from 2nm thick film became much bigger. The self-assembled structure has very different shape and sizes depending on the substrate and temperatures and so on. [44]

Chapter 5: EXPERIMENTAL RESULT

Enhanced Optical Properties

In the previous chapters, the optical properties of the organic field effect transistor and the gold nanoparticle were mainly investigated. It was confirmed that the absorption spectra peak and the spectral response peak of the organic field effect transistor were determined by the difference between the HOMO energy level and the LUMO energy level of the organic material, P3HT. It was also confirmed that the surface plasmon resonance peak and the absorption spectra peak were determined by the size and shape of the gold nanoparticles.

In this chapter, the surface plasmon resonance effect of the gold nanoparticles is applied to the optical and electrical properties of the organic field effect transistor. The electrical and optical properties have been investigated to compare with a device without plasmonic nanostructure. For the spectral response measurement of the organic field effect transistor deposited with gold nanoparticles, the SR830 Lock-In Amplifier and the SR540 Optical Chopper were used because noise signals had to be removed.

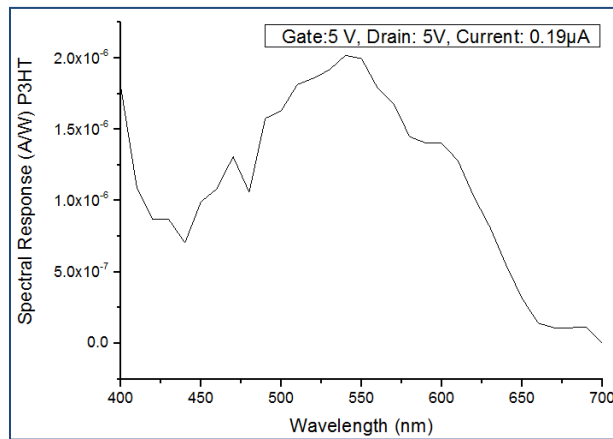


Figure 5.1 The spectral response curve of the OFET at Gate Voltage: 5V, leakage: $0.00117 \mu\text{A}$, Drain-Source Voltage: 5V and Drain-Source Current: $0.19 \mu\text{A}$.

Since the localized surface plasmon resonance is electron dominant effect. The transistor needs to be operated as an n-type material. Fortunately, we have observed that the P3HT transistor is working under weak positive gate bias, even though it has a very small drain current. This positive gate bias can create a attracting force to the hot electrons generated in the gold nanostructure structure. The spectral response curve of the organic field effect transistor was measured at Gate Voltage: 5V, leakage: $0.00117\mu\text{A}$, Drain-Source Voltage / Current: 5V / $0.19\mu\text{A}$. The measurement value at the peak is $2.02\mu\text{A/W}$ as shown in Figure 5.1.

The same condition, Gate Voltage: 5V and Drain-Source Voltage: 5V, was used for the spectral response measurement of the organic field effect transistor deposited with gold nanoparticles. The measurement value is the voltage as shown in Figure 5.2.

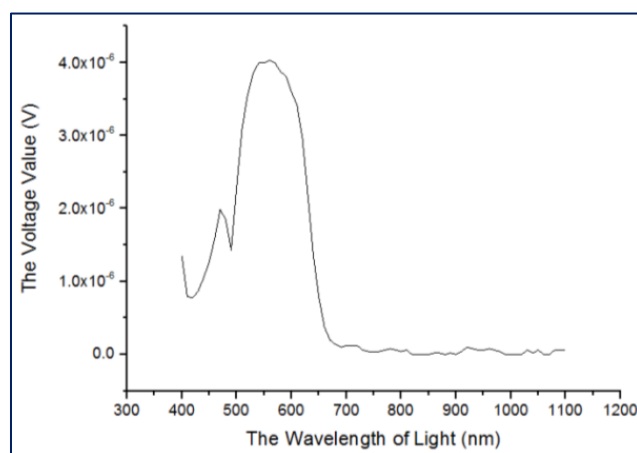


Figure 5.2 Voltage value for spectral response of the organic field effect transistor deposited with gold nanoparticles.

But the spectral response is the current generated per the power incident. Voltage is divided by the resistor (65K ohm) and current value is obtained as shown in Figure 5.3.

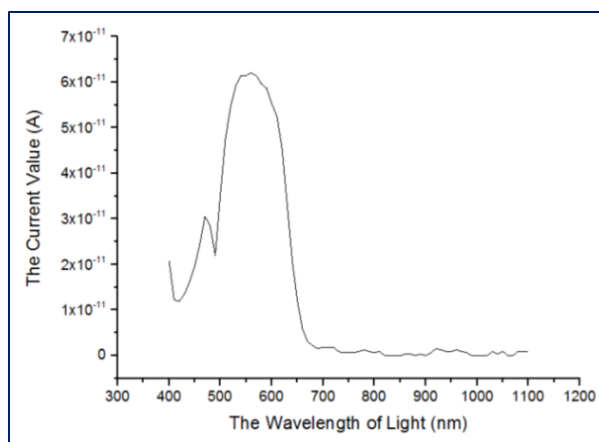


Figure 5.3 The current value for spectral response of the organic field effect transistor deposited with gold nanoparticles.

The power of monochromatic light for the halogen lamp was obtained by using a reference solar cell. The current value of the organic field effect transistor deposited by gold nanoparticles was divided by the power of the halogen lamp and the spectral response was measured as shown in Figure 5.4.

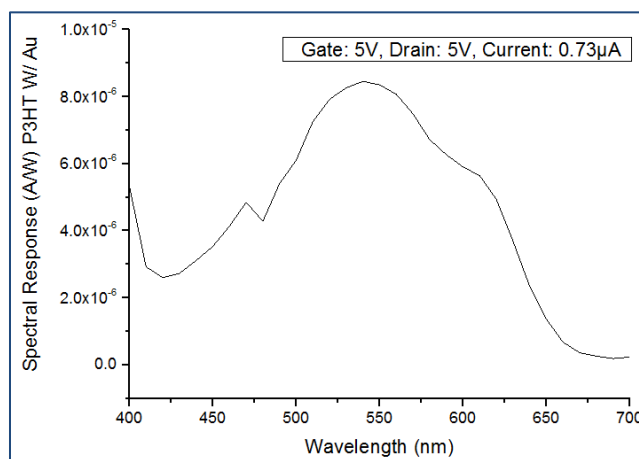


Figure 5.4 The spectral response curve of the organic field effect transistor deposited with gold nanoparticles at Gate Voltage: 5V, Drain-Source Voltage/Current: 5V/ 0.73 μ A.

The optical properties have been investigated to compare with a device without

plasmonic nanostructure. In Figure 5.1, the measurement value of a spectral response peak for the organic field effect transistor is $2.02\mu\text{A/W}$. In Figure 5.4, the spectral response for the organic field effect transistor deposited with gold nanoparticles is $8.45\mu\text{A/W}$ at the same gate and drain-source voltage.

The gold nanoparticles incorporated in organic transistor shows improved drain current from $0.19\mu\text{A}$ to $0.73\mu\text{A}$ due to the increased conductivity assisted by the free electrons in the metal nanoparticles. Drain Voltage was decreased to avoid the electrical effect. The enhanced photo-responsivity (A/W) was also observed in its optical detector operation.

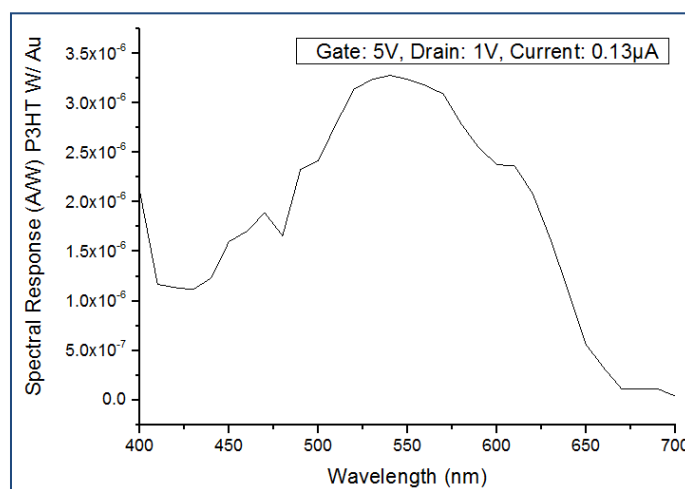


Figure 5.5 The spectral response curve of the organic field effect transistor deposited with gold nanoparticles at Gate Voltage: 5V, Drain-Source Voltage: 1V and Drain-Source Current: $0.13\mu\text{A}$.

In Figure 5.5, the measurement value of a spectral response peak for the organic field effect transistor deposited with gold nanoparticles is $3.28\mu\text{A/W}$ at drain-source current $0.13\mu\text{A}$. The measurement value with gold nanoparticles is increased by 1.62 times than the measurement value without gold nanoparticles as shown in Figure 5.6.

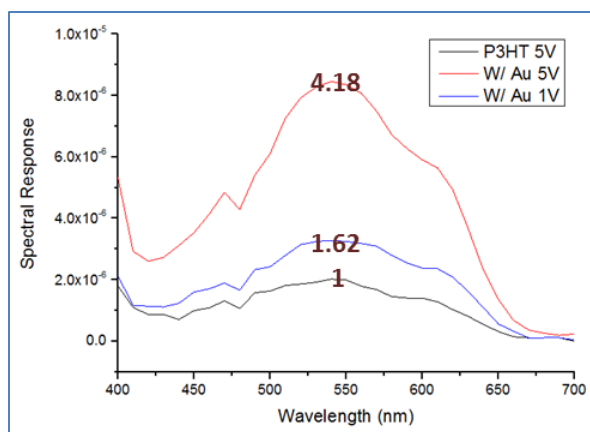


Figure 5.6 The spectral responses at 5V gate voltage without gold nanoparticles and at 5V and 1V gate voltage with gold nanoparticles.

It is possible that the surface plasmon resonance of the gold nanoparticles is transferred to the organic materials through the interface between the metal and the dielectric. A slight change of the spectral response was observed and we believe that this is originated from the contribution of the plasmon induced hot electrons in the metal nanoparticles as shown in Figure 5.7.

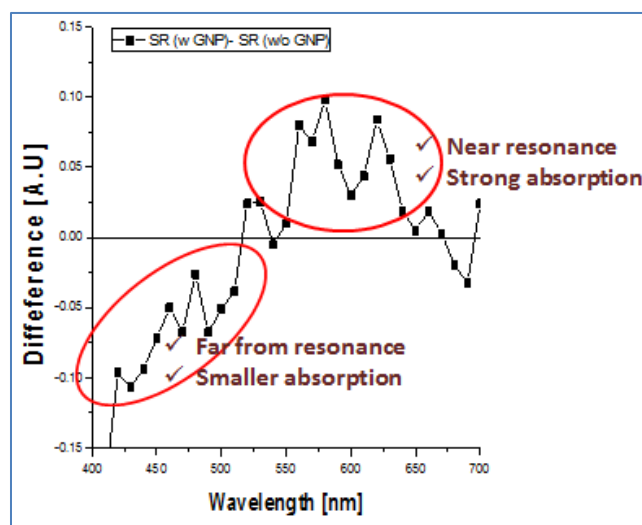


Figure 5.7 The difference of the normalized spectral response between the OFETs with gold nanoparticles and without gold nanoparticles.

For the gold nanoparticles assembled from 2nm thick film, the surface plasmon resonance phenomena cause absorption of light around 600nm wavelength. At 550~650nm wavelength, free electrons of the metal surface directly go to organic material because of the strong absorption around the wavelength of the surface plasmon resonance as shown in Figure 5.8. Thus, increased spectral response can be observed.

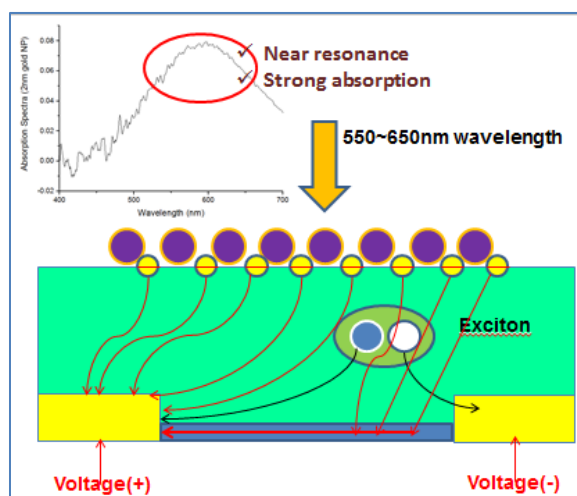


Figure 5.8 The process of charge transfer at 550~650nm wavelength.

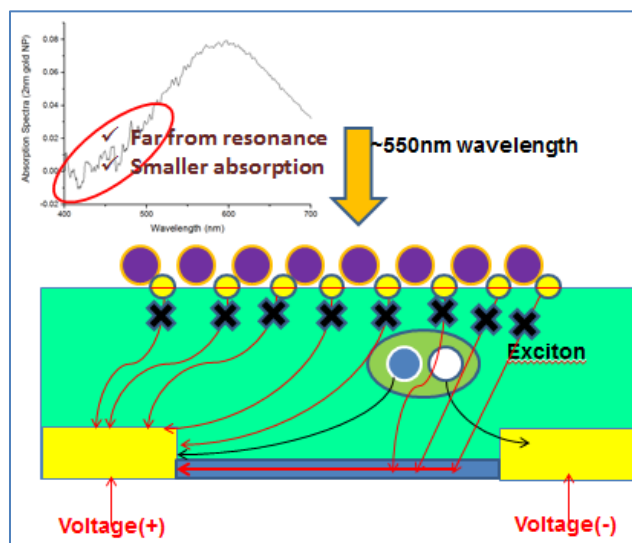


Figure 5.9 The process of charge transfer below 550nm wavelength.

Below 550nm wavelength, free electrons of the metal surface do not go to organic material because of the smaller absorption as shown in Figure 5.9. But rather spectral response was decreased due to the decreased absorption in P3HT by the absorption of gold nanoparticles. It was successfully demonstrated that the improved optical properties of the OFETs are due to surface plasmon resonance of the metal nanoparticles.

Enhanced Electrical Properties

In addition to the enhanced optical properties, electrical properties were enhanced by gold nanoparticles. The resistance of organic field effect transistor is lowered by coating gold nanoparticles on the organic material. The core of organic field effect transistors is to create organic materials with good electrical characteristics. One of the good characteristics is to reduce the leakage by gate voltage and increase drain-source. In order to increase the current, if drain-source voltage is increased, the organic material's viability is degraded. However, it is possible to increase the current by coating gold nanoparticles without increasing the current drain-source voltage.

When the gold nanoparticles were produced from 2nm thick gold film, the drain-source current of the OFET was increased up to 3.84 times at the same gate and drain-source voltage. The measurement value of drain-source current for the organic field effect transistor is $0.19\mu\text{A}$ and the drain-source current for the organic field effect transistor deposited with gold nanoparticles is $0.73\mu\text{A}$ at 5V gate voltage and 5V drain-source voltage as shown in Figure 5.10. The hybridization using polymer semiconducting materials and metal nanoparticles can provide improved mobility due to the free electron concentration in the metal nanostructure.

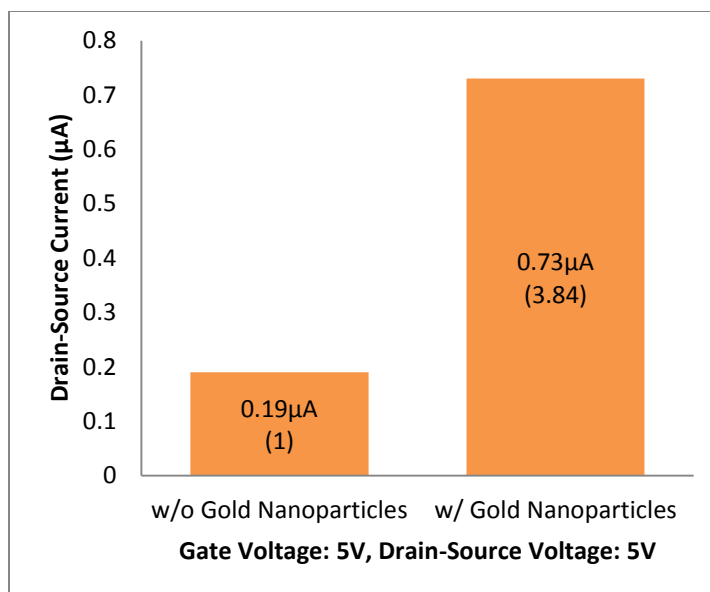


Figure 5.10 The enhanced drain-source current of the OFET up to 3.84 times with gold nanoparticles at 5V gate voltage and 5V drain-source voltage.

The leakage by gate voltage can be minimized by adjusting drain-source voltage. Increasing gate voltage, leakage occurs more. But, it was confirmed through the organic field effect transistor coated with gold nanoparticles that the condition to minimize leakage is determined not only by gate voltage but also by drain-source voltage. The leakage is not simply reduced by increasing the drain-source voltage. As the drain-source voltage of 5V, 10V, and 20V was applied to the organic field effect transistor respectively, the leakage became a minimum value at 10V. The leakage was increased at 5V or 20V. In case appropriate drain-source voltage is applied to the organic field effect transistor, the leakage can be minimized. It can be estimated that the electrons flowing between the drain and the source attract the electrons flowing from an electrode into the gate. It is a kind of laminar flow. This effect depends on the channel width of the electrodes and the channel length between the electrodes.

Chapter 6: SUMMARY and FUTURE WORK

Summary

We have successfully demonstrated a hybrid organic thin film transistor device with enhanced optical detection and electrical properties. An organic field effect transistor using P3HT as an active material was prepared for the experiment and gold nanoparticles were deposited using a thermal reflow method using a vacuum evaporated thin gold film.

The gold nanoparticles incorporated in organic transistor shows the enhanced electrical property due to the increased conductivity assisted by the free electrons in the metal nanoparticles, and the enhanced photo responsivity (A/W) and a slight change of the spectral response as shown in Figure 6.1 because of the contribution of the surface plasmon resonance induced hot electrons in the metal nanoparticles.

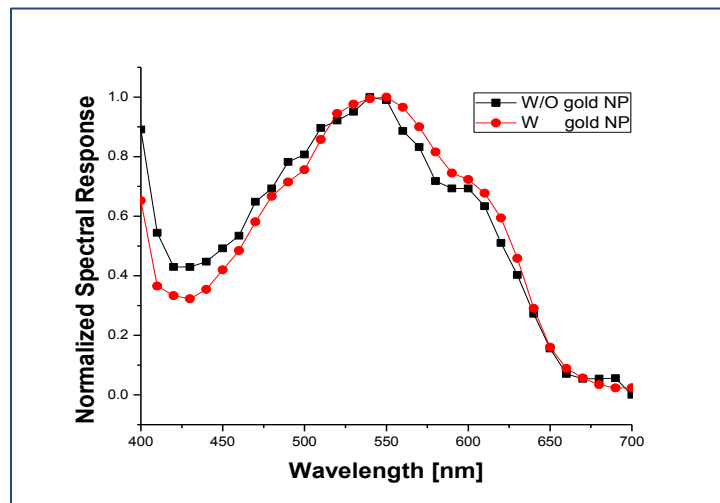


Figure 6.1 The normalized spectral response of the OFET with and without Au NP.

At 550~650nm wavelength, free electrons of the metal surface have the strong absorption. Thus, enhanced spectral response is observed around the wavelength of the

surface plasmon resonance. Below 550nm wavelength, the decreased spectral response is obtained because free electrons of the metal surface have smaller absorption and the amount of light absorption by organic semiconductor is decreased due to the absorption of light by the gold nanoparticles on the surface of the OFET. This work showed a feasibility for the direct collection of plasmon induced hot electrons through organic semiconducting material.

Important Consideration and Future Work

Organic semiconductor, P3HT, was spin coated on the silicon wafer at the speed of 1200rpm for 30 seconds. The thickness of the P3HT is more than 100nm with the spin speed and time. P3HT was thicker than the thickness of the gold nanoparticles. Thus, large portion of light was absorbed by the P3HT compared with gold nanoparticles. When the absorption rate is increased by the thickness of the organic material, then the recombination rate of electron and hole inside of organics also increases and the absorption rate of metal nanoparticles decreases compared with the absorption rate of the organic material. Hence, the thickness of the organic semiconductor should be reduced by adjusting spin speed and time.

The Difference between the HOMO energy and the LUMO energy of P3HT is 1.9eV. The minimum wavelength of the light absorbed by P3HT is 652nm and the wavelength of the absorption spectra peak is 550nm. The absorption property of P3HT is consistent with the energy level gap of P3HT. The surface plasmon resonance peak is around 550nm~600nm. The absorption spectra peak of P3HT overlapped with the surface plasmon resonance peak. In this case, it is hard to detect the distinct characteristic of surface plasmon resonance. PVK as organic material, HOMO: 5.8eV, LUMO: 2.2eV, the

wavelength of the absorption spectra peak: 450~500nm, is better to sense the change of the spectral response by plasmonic nanostructure.

N-type organic semiconductors instead of p-type organic materials are suitable for checking the charge transfer. The applied drain voltage and gate voltage are positive to attract the charge due to the charge is negative. In case of the n-type organic materials can make the channel better at the positive gate voltage.

Through these results, the hybridization using polymer semiconducting materials and metal nanoparticles can be applied to the infrared detector. For example, the organic semiconductors such as P3HT, the difference between HOMO and LUMO energy level is below 1.9eV, do not show any spectral response by infrared light. If the gold nano rods, which have the surface plasmon resonance peak of 800nm wavelength, are deposited onto the surface of the P3HT organic transistor, the device can absorb infrared light and show spectral response around 800nm wavelength. The enhanced optical properties of organic material by surface plasmon resonance of metal nanoparticles will contribute to make very sensitive with organic materials.

References

- [1] Riordan, M. and L. Hoddeson (1997). "Crystal fire: the birth of the information age." New York, Norton.
- [2] SHIVE, J. N. (1950). "The phototransistor." Bell Laboratories Record. May 1950.
- [3] Chiang, C. K., et al. (1977). "Electrical conductivity in doped polyacetylene." Physical Review Letters 39(17): 1098-1101.
- [4] Ebisawa, F., et al. (1983). "Electrical properties of polyacetylene / polysiloxane interface." Journal of Applied Physics 58(6): 3255-3259.
- [5] Ziemelis, K. (1998). "Putting it on plastic." Nature 393(6686): 619-620.
- [6] Reese, C. and Z. Bao (2007). "Organic single-crystal field-effect transistors." Materials Today 10(3): 20-27.
- [7] Sherry, L. J., et al. (2005). "Localized surface plasmon resonance spectroscopy of single silver nanocubes." Nano Letters 5(10): 2034-2038.
- [8] Kwon, M.-K., et al. (2008). "Surface-plasmon-enhanced light-emitting diodes." Advanced Materials 20(7): 1253-1257.
- [9] Ryu, H., et al. (2008). "Effect of Sr substitution on photoluminescent properties of BaAl₂O₄:Eu²⁺, Dy³⁺." Physica B: Condensed Matter 403(1): 126-130.
- [10] Hayakawa, T., et al. (1999). "Enhanced fluorescence from Eu³⁺ owing to surface plasma oscillation of silver particles in glass." Journal of Non-Crystalline Solids 259(1): 16-22.
- [11] Ozbay, E. (2006). "Plasmonics: merging photonics and electronics at nanoscale dimensions." Science (New York, N.Y.) 311(5758): 189-193.
- [12] Bohren, C. F. and Huffman, D. R. (1983). "Absorption and scattering of light by small particles." New York, Wiley.
- [13] Cho, C., et al. (2011). "Enhanced optical output power of green light-emitting diodes by surface plasmon of gold nanoparticles." Applied Physics Letters 98(5): 051106-051106-051103.
- [14] Barnes, W. L., et al. (2003). "Surface plasmon subwavelength optics." Nature 424(6950): 824-830.
- [15] "Organic chemistry." <http://blog.naver.com/yhs3480/>.

- [16] "Chemguide." <http://www.chemguide.co.uk/>.
- [17] "Supplement information." <http://blog.naver.com/olta2/>.
- [18] "Sigma and pi bonding." <https://sites.google.com/site/ed350201003/Task/>.
- [19] "Organic semiconductor world." <http://www.iapp.de/orgworld/>.
- [20] Heeger, A. (2001). "Nobel lecture: semiconducting and metallic polymers: the fourth generation of polymeric materials." *Reviews of Modern Physics* 73(3): 681-700.
- [21] Forrest, S. R. (2004). "The path to ubiquitous and low-cost organic electronic appliances on plastic." *Nature* 428(6986): 911-918.
- [22] Köhler, A. (2012). "Organic semiconductors: no more breaks for electrons." *Nature Materials* 11(10): 836.
- [23] Sze, S. M. (1981). "Physics of semiconductor devices." New York, Wiley.
- [24] Pesavento, Paul V., et al. (2004). "Gated four-probe measurements on pentacene thin-film transistors: contact resistance as a function of gate voltage and temperature." *Journal of Applied Physics* 96(12): 7312-7324.
- [25] Helander, M. G., et al. (2008). "Band alignment at metal / organic and metal / oxide / organic interfaces." *Applied Physics Letters* 75(19): 193310-193310-193313.
- [26] Siol, C., et al. (2008). "Electron trapping in pentacene based p- and n-type organic field-effect transistors." *Applied Physics Letters* 75(13): 133303-133303-133303.
- [27] Geddes, C. D. and Lakowicz, J. R. (2002). "Editorial: metal-enhanced fluorescence." *Journal of Fluorescence* 12(2): 121-129.
- [28] Aslan, K., et al. (2005). "Annealed silver-island films for applications in metal-enhanced fluorescence: interpretation in terms of radiating plasmons." *Journal of Fluorescence* 15(5): 643-654.
- [29] Knoll, W. (1998). "Interfaces and thin films as seen by bound electromagnetic waves." *Annual Review of Physical Chemistry* 49(1): 569-638.
- [30] Sohn, S. H., et al. (2009). "Effects of the surface coating of BaMgAl₁₀O₁₇:Eu²⁺ phosphor with SiO₂ nano-particles." *Journal of Luminescence* 129(5): 478-481.
- [31] Noguez, C. (2007). "Surface plasmons on metal nanoparticles: the influence of shape and physical environment." *Journal of Physical Chemistry C* 111(10): 3806-3819.

- [32] Camley, R. E. (1984). "Collective excitations of semi-infinite superlattice structures: surface plasmons, bulk plasmons, and the electron-energy-loss spectrum." *Physical Review B* 29(4): 1695-1706.
- [33] Maier, S. A. (2007). "Plasmonics: fundamentals and applications." New York, Springer.
- [34] Xia, Y. and Halas, N. J. (2005). "Shape-controlled synthesis and surface plasmonic properties of metallic nanostructures." *MRS Bulletin* 30(5): 338-348.
- [35] Jain, J. K. and Allen, P. B. (1985). "Predicted Raman intensities for bulk and surface plasmons of a layered electron gas." *Physical Review Letters* 54(9): 947-950.
- [36] Shimizu, T., et al. (2003). "Size evolution of alkanethiol-protected gold nanoparticles by heat treatment in the solid state." *The Journal of Physical Chemistry B* 107(12): 2719-2724.
- [37] Park, Y. D., et al. (2006). "Energy-level alignment at interfaces between gold and poly(3-hexylthiophene) films with two different molecular structures." *Electrochemical and Solid-State Letters* 9(11): G317.
- [38] "Dnanotech." <http://www.dileepnanotech.com/>.
- [39] Torsi, L., et al. (2013). "Organic field-effect transistor sensors: a tutorial review." *Chemical Society reviews* 42(22): 8612.
- [40] Turkevich, J., et al. (1951). "A study of the nucleation and growth processes in the synthesis of colloidal gold." *Discussions of the Faraday Society* 11: 55.
- [41] Link, S. and El-Sayed, M. A. (1999). "Size and temperature dependence of the plasmon absorption of colloidal gold nanoparticles." *The Journal of Physical Chemistry B* 103(21): 4212-4217.
- [42] "Sigma-Aldrich." <http://www.sigmaaldrich.com/>.
- [43] "Cytodiagnosics." <http://www.cytodiagnosics.com/>.
- [44] Yazid, H., Adnan, R., Hamid, S. A. and Farrukh, M. A. (2010). "Synthesis and characterization of gold nanoparticles supported on zinc oxide via the deposition-precipitation method." *Turk J Chem* 34: 639-650.